PHILOSOPHICAL TRANSACTIONS OF THE ROYAL SOCIETY A MATHEMATICAL, PHYSICAL & ENGINEERING SCIENCES

The Geology of Longonot Volcano, Central Kenya: A Question of Volumes

S. C. Scott

Phil. Trans. R. Soc. Lond. A 1980 **296**, 437-465
doi: 10.1098/rsta.1980.0188

THE GEOLOGY OF LONGONOT VOLCANO, CENTRAL KENYA: A QUESTION OF VOLUMES

BY S. C. SCOTT

School of Environmental Sciences, Plymouth Polytechnic, Drake Circus, Plymouth PL4 8AA, U.K.

(*Communicated by P. Allen, F.R.S. – Received* 14 *December* 1978 *– Revised* 29 *May* 1979)

[Plates 1–4; pullout 1]

CONTENTS

 [Published 14 March 1980

The Quaternary central volcano Longonot is situated on the floor of the Eastern Rift Valley of Kenya, at 36°26′E, 0°55′S, within the Nakuru–Naivasha peralkaline volcanic province. The volcano consists of peralkaline trachyte lavas and pyroclastics, accompanied by minor volumes of mixed, hawaiite–peralkaline trachyte lavas. Longonot has been mapped in detail as a prerequisite to the collection of a sample suite representative of the volumes of liquid erupted during specific periods of activity. Particular emphasis has been given to establishment of the time relations and original volumes of its volcanic products.

Seven episodes of activity are recognized:

(i) growth of a primitive, peralkaline trachyte composite cone (280 km^3);
(ii) caldera collapse at the summit of the composite cone, accompanied by late-stage pyroclastic activity (> 50 km^3);
(iii) eruption of mixed, hawaiite–peralkaline trachyte lavas on the northern Longonot plains (0.5 km^3);
(iv) growth of a peralkaline trachyte lava-pile on the partly infilled, eastern caldera floor (16 km^3);
(v) lava-pile growth terminated by a phase of ash eruptions (> 2 km^3); asymmetric collapse of the lava-pile and ash-cover summit followed, forming a pit crater;
(vi) eruption of very recent, mixed hawaiite–peralkaline trachyte lava onto the pit-crater floor (> 0.34 km^3);
(vii) flank eruptions of two peralkaline trachyte flows (0.045 km^3).

Liquid equivalent volumes of volcanic products erupted during each episode of activity are calculated; the results indicate that the products formed from the greater part of the total liquid volume erupted are not exposed. This presents a serious problem for the collection of a sample suite representative of the volumes of liquid erupted throughout the entire history of the volcano. A sample suite truly representative of liquid volumes erupted can only be collected from those products erupted during and after the late-stage caldera pyroclastic activity. These products, however, account for only 14.5% of the total liquid volume. This unavoidable undersampling must be taken into account when the petrogenesis of the entire Longonot volcanic succession is considered.

1. Introduction

The Quaternary peralkaline trachyte volcano Longonot is situated southeast of Lake Naivasha, on the floor of the Gregory Rift Valley, Central Kenya, at 36° 26′ E, 0° 55′ S (figure 1). The Rift Valley lies along the north–south axis of the 'Kenya Dome', a regional crustal upwarp, 500 km in diameter, centred on the Nakuru area, 80 km north of Longonot (Baker & Wohlenberg 1971). The volcano is one of a series of Quaternary centres on the Rift Valley floor, which includes, from north to south, Menengai, Eburru, southwest Naivasha and Suswa, and which

collectively form the Quaternary peralkaline volcanic province of Central Kenya (see figure 1). The geochemistry of individual centres in this young, compact and easily accessible province is currently being investigated in an attempt to increase our understanding of the petrogenesis of peralkaline magmas within continental regions, subject to anorogenic crustal upwarping and rifting. A geochemical study of the Longonot volcanic succession forms an integral part of this investigation.

However, in any study of the geochemistry of volcanic rocks erupted from a given centre, the sampling technique employed is of the utmost importance. Walker (1973) points out that methods such as grid sampling, random sampling or complete sampling of a few vertical sections all generally introduce a bias owing to:

(i) the three main types of volcanic product, lava flows, ignimbrites and fall deposits, being transported to different distances from the vent, and

(ii) their different survival ratings when subjected to erosion causing a change in the original volume relations of the volcanic products.

Walker makes a plea to geochemists to undertake detailed mapping of a volcano prior to sampling, to establish the time relations and original volumes of its products. The volumes of liquid that gave rise to the original volumes of volcanic products erupted during specific stratigraphic periods can then be calculated, permitting the collection of a sample suite that is representative of the liquid volume erupted during each of the stratigraphic periods. Such an approach, Walker argues, would give a clearer insight into the chemical evolution of the liquid erupted from the volcano. In addition, cycles of activity and temporal variations in the style of eruption, identified from volcanological evidence, can be used as an extra aid to the interpretation of geochemical data.

Although Longonot is mentioned in the works of Gregory (1896, 1920, 1921), these early references do not contribute significant information on the geology of the volcano. Longonot is featured in the *Catalogue of active volcanoes and solfatara fields of Africa and the Red Sea* (Richard & Van Padang 1957), but only brief mention is made of the form and structure of the volcano and no information relating to the volcanic history of the centre is offered. Thompson & Dodson (1963), in their report on the geology of the Naivasha region, mention the general morphology of the volcano and the rock types exposed, but again give very little information on the volcanic history of the centre. Their map of the Naivasha region, at a scale of 1:125000, includes Longonot in the southwest corner, but the small scale precludes any detailed representation of the geology. Consequently, detailed time and volume relations of the volcanic products cannot be deduced. Longonot is also mentioned by McCall (1967), who points out the existence of an earlier volcano within an embayed summit caldera containing a later secondary volcano. This secondary volcano forms the present upstanding, terraced lava pile visible from Lake Naivasha and the Nairobi–Naivasha road.

With reference to Walker's (1973) comments, the lack of detailed information on the volcanic succession at Longonot made detailed geological mapping necessary to provide a sound volcanological basis for the collection of a sample suite representative of the volumes of liquid erupted during specific stratigraphic periods. This paper presents the results of the mapping.

Longonot covers an area of 500 km². Pyroclastic products, especially airfall ash, are spread over a much larger area, probably of the order of 3000 km². The volcano rises to a maximum altitude of 2780 m above sea level, *ca.* 1000 m above the south-sloping rift floor, which ranges

PHILOSOPHICAL TRANSACTIONS OF THE ROYAL SOCIETY A MATHEMATICAL, PHYSICAL & ENGINEERING SCIENCES

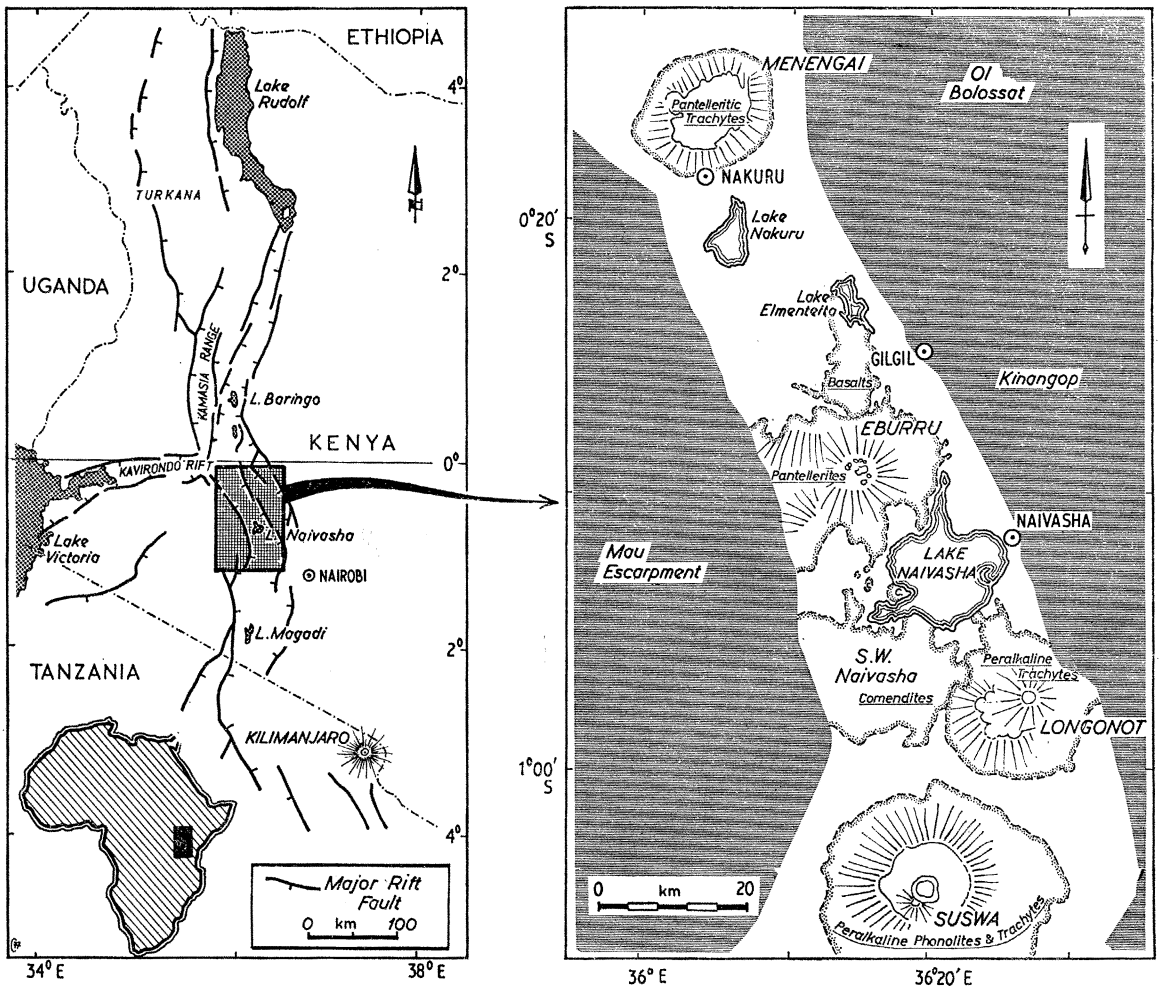

FIGURE 1. Location of Longonot within the Quarternary peralkaline volcanic province of Central Kenya. The location and composition of the major central volcanoes Menengai, Eburru, Longonot and Suswa and of the lava field of southwest Naivasha are shown. Townships of Nakuru, Gilgil and Naivasha are also indicated.

in altitude from 1700 m south of the volcano to 1850 m north of the volcano. Exposures of all but the very recent lavas are restricted to flow margins, the lava surfaces being completely covered by young airfall ash. Exposures of pyroclastic rocks are restricted to the walls of erosion gullies.

2. General outline of volcanic history

Peralkaline trachyte lava flows, mixed hawaiite–peralkaline trachyte lava flows, and peralkaline trachyte pyroclastic rocks form the Quaternary volcano of Longonot.

The Longonot succession is divided into seven major eruptive episodes as follows:

(i) Growth, on the south-sloping rift floor, of an early peralkaline trachyte composite volcano *ca.* 30 km basal diameter and of late Pleistocene age.

(ii) Collapse of the summit region to form a large embayed caldera. Syn- and post-collapse eruptions from within the caldera depression produced a thick, widely distributed succession of

THE VOLCANIC GEOLOGY OF MOUNT LONGONOT, CENTRAL KENYA

S.C. Scott, 1979

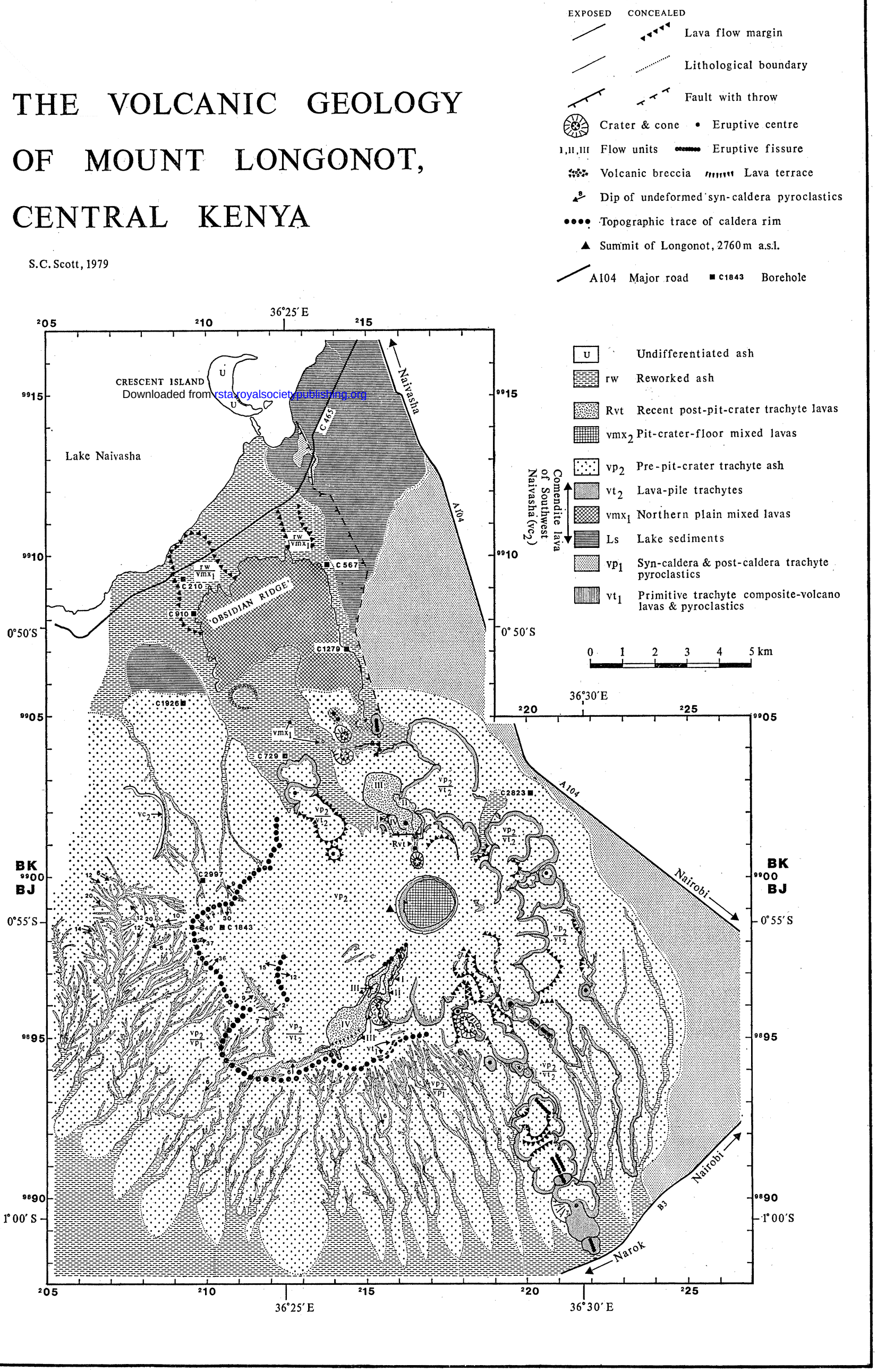

FIGURE 2.

THE VOLCANIC GEOLOGY OF MOUNT LONGONOT, CENTRAL KENYA

S.C. Scott, 1979

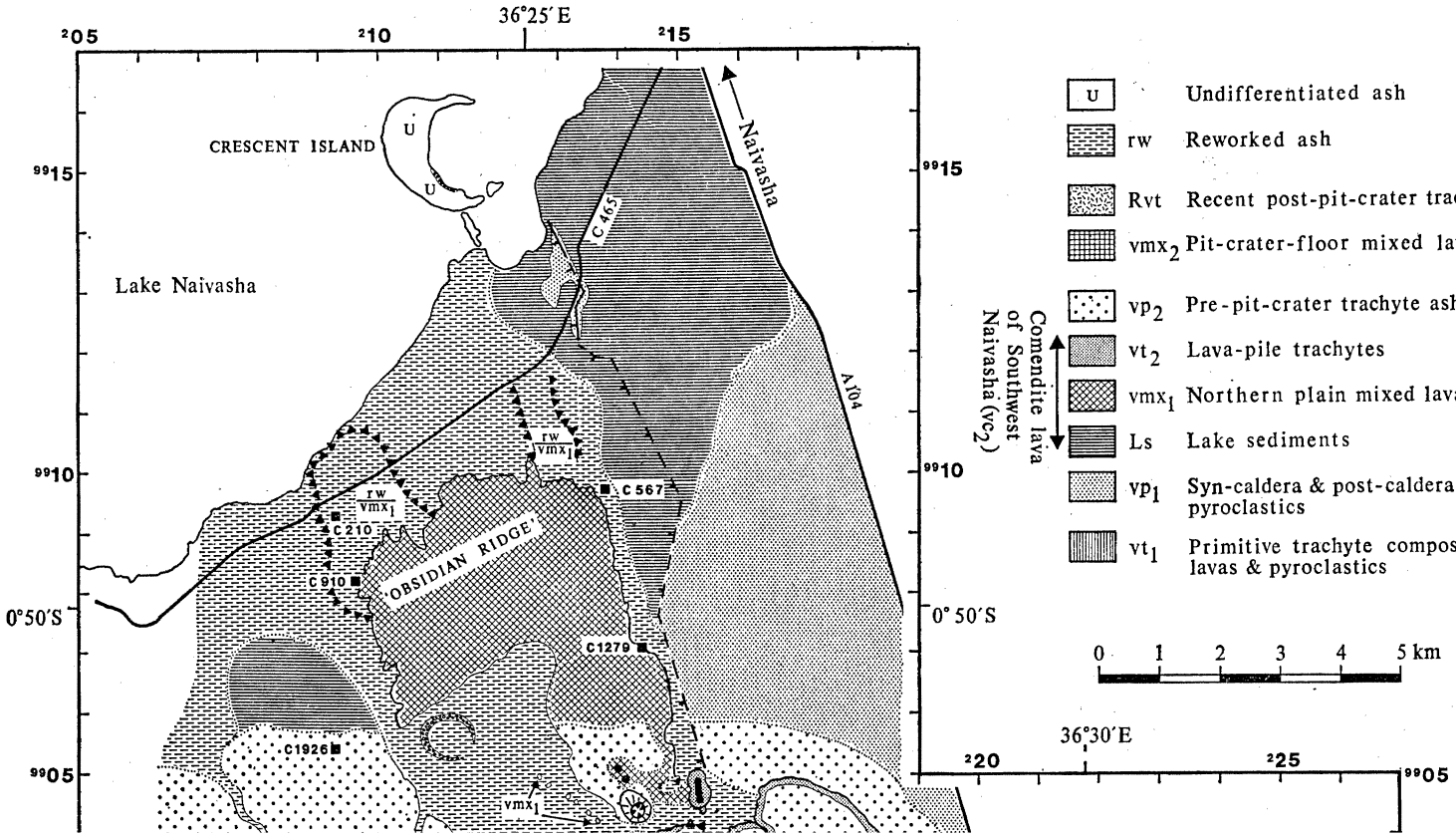

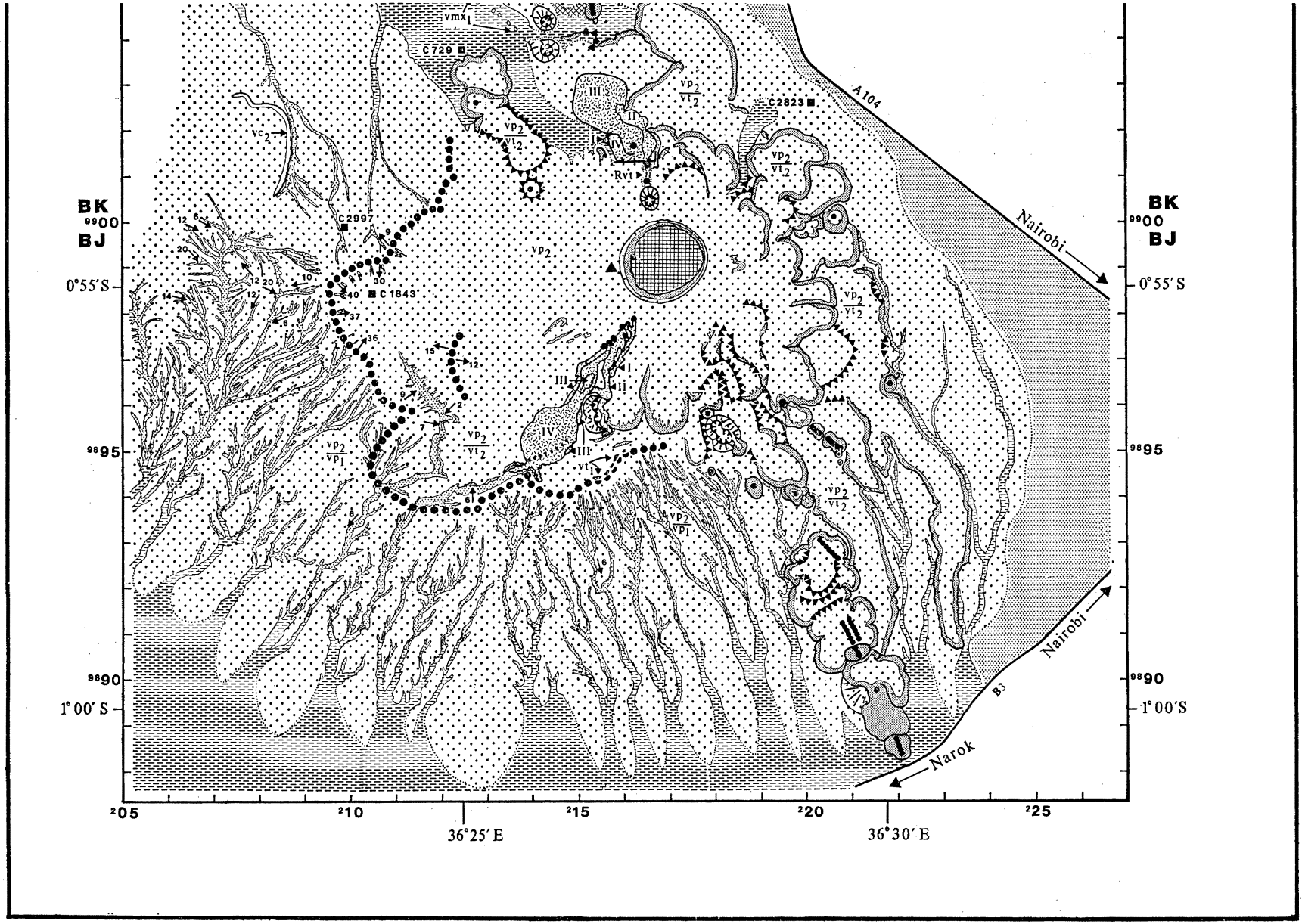

FIGURE 2.

pyroclastic deposits, that mantle the composite volcano slopes and almost wholly infill the caldera depression.

(iii) Lateral eruption of Early Holocene, mixed hawaiite–peralkaline trachyte lava flows onto the pyroclastic-mantled northern slopes of the composite volcano.

(iv) Growth of a peralkaline trachyte lava-pile from a source region situated on the infilled, eastern caldera floor.

(v) Effusive activity finally gave way to strong explosive activity, which produced a thick deposit of ash and pumice covering much of the lava-pile succession. Asymmetric collapse of the ash-mantled lava-pile summit region followed, forming a circular pit crater 1.8 km in diameter.

(vi) Eruption of mixed, hawaiite–peralkaline trachyte lavas onto the pit-crater floor.

(vii) Lateral eruption of two peralkaline trachyte lava flows, *ca.* 200–300 a B.P. (years before present), from radial fissures centred on the pit-crater collapse. Fumarolic activity persists at the present day and is confined to the base of the pit-crater wall.

The detailed eruptive history of the volcano is described in the following sections. Throughout the description, calculations are presented for the approximate original total volume of volcanic products erupted during each episode of activity. Where such a volume cannot be calculated, a minimum value is quoted. Assumptions made to simplify the form of the complex rock bodies being considered are listed prior to the volume calculations. The distribution of rock units at Longonot is shown on figure 2, while the location of boreholes and important volcanological features mentioned in the text are shown on figure 3.

3. The primitive composite volcano

The earliest recognizable volcanic structure at the Longonot centre is a large composite volcano, a remnant of which occurs in the south and southwest parts of the region, in an area outlined by grid references BJ210890, BJ050910, BJ100980 and BJ180950 (see figure 3). It appears as a sector of a cone displaying a concave profile, rising from 1700 m in the south and southwest to 2200 m in the north and northeast, where it is abruptly terminated by a steep, embayed caldera wall. The cone slopes and western caldera wall are completely mantled by younger syn- and post-caldera pyroclastics.

Part of the internal structure of the composite volcano is, however, exposed in the north-facing wall of the caldera between BJ160950 and BJ153944 (see figure 3). The succession is:

10 m	Dark grey to green, vesiculated, flow banded, porphyritic, peralkaline trachyte lava containing small, sparse phenocrysts of alkali feldspar and variable quantities of xenoliths, both cognate and foreign. Vesicles are lenticular, with their long axes ranging from 0.5 mm to 1.0 m. Scoriaceous surface contains encrustations of Trona.
0.5 m	Angular obsidian lapilli (*ca.* 10%), crystalline lava lapilli (*ca.* 5%) and angular pumice lapilli (*ca.* 65%) in a coarse, semi-indurated, light yellow, sandy ash matrix.
0.5 m	Fine, orange ash, containing *ca.* 20% angular obsidian, pumice and lava lapilli.
0.3 m	Homogeneous, light grey, well sorted pumice deposit, containing *ca.* 10% angular obsidian and crystalline lava lapilli.

The lava and pyroclastics dip 20–25° at 140°, i.e. down the primitive volcano slope.

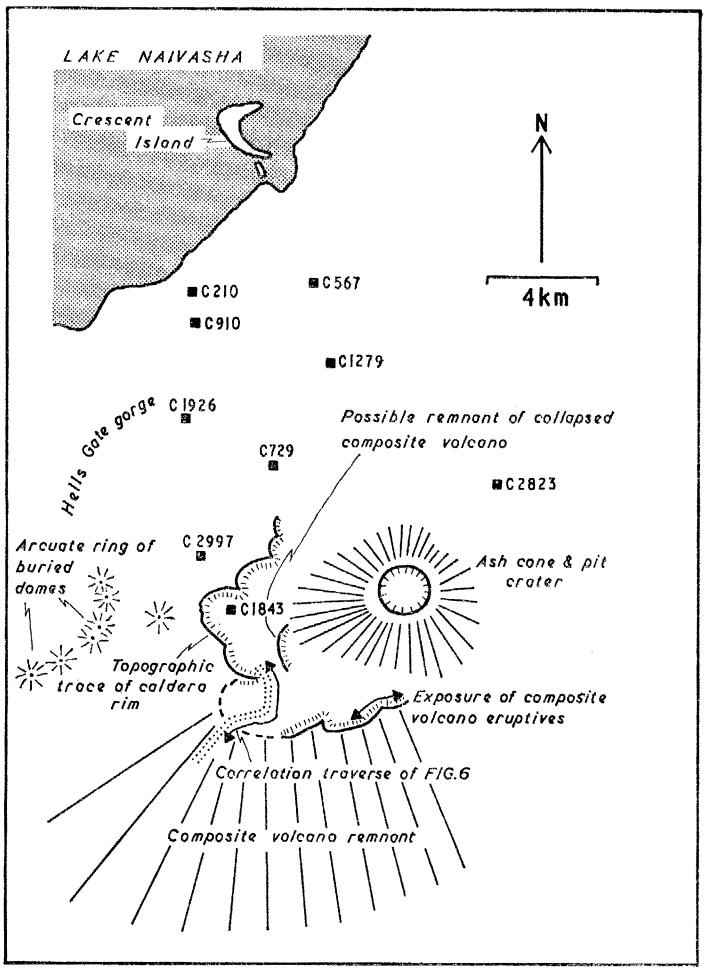

FIGURE 3. Sketch map showing the locations of important volcanological features and boreholes. Location of boreholes indicated by filled squares.

An additional section through the internal structure is presented in the drill log of borehole C2997, sunk by the Kenya Ministry of Agriculture (Water Development Department) into the northwestern slopes of the cone at BJ099999 (see table 1 and figure 3). As the hole has been sunk directly into a thin horizon of pre-pit-crater ash overlying syn-and post-caldera pyroclastics that mantle the cone, the initial 140 m of 'volcanic ash and pumice' is interpreted as a section through these pyroclastics. The thick, alternating 'broken trachyte lava' and 'volcanic ash' horizons are interpreted as being a section through the underlying cone structure. The caldera wall exposure indicates that the 'volcanic ash' horizons recorded in the borehole log are made up of several individual beds. These two lines of evidence demonstrate the composite form of the primitive volcano.

The dimensions of the composite-volcano remnant suggest a basal diameter of *ca.* 30 km for the primitive cone. Projection of the cone slope beyond the caldera scarp in the west and south indicates that the pre-caldera cone reached no higher than 3000 m a.s.l., 1200 m above the average altitude of the south-sloping rift floor. Assuming a perfect conical form, then

$$\text{volume of composite volcano} = \tfrac{1}{3} \times 15^2 \times \pi \times 1.2 \text{ km}^3 = \mathbf{280\ km^3} \text{ (to nearest 10 km}^3\text{)}.$$

The base of the composite cone is not exposed and so its age relative to the youngest flood lavas of the rift floor, the Pleistocene Plateau Trachyte series (Baker 1958), cannot be directly demonstrated. However, to the south, the earliest lava flows of the primitive Mount Suswa shield directly overlie faulted Lower Pleistocene Plateau Trachytes (Johnson 1969). Shackleton (1955) and Baker (1958) consider the fault movements to have ended before the Upper Pleistocene. As most of the early Suswa flows are not cut by major faults, they are taken by Johnson (1969) to be Upper Pleistocene in age. The primitive cones of Longonot and Suswa are about the same size and are mantled by syn-caldera pyroclastics in a similar state of erosion on both volcanoes. Although indirect, this approach suggests that the primitive Longonot composite volcano and the primitive Suswa shield were active contemporaneously. More recently, Baker & Mitchell (1976) have given an age of 0.4 Ma for the termination of major faulting of the Plateau Trachyte series. Such evidence implies a maximum of 0.4 Ma B.P. for the commencement of activity at Suswa and Longonot.

Growth of the primitive Longonot composite cone, along with eruption of the early comendite volcanics of the southwest Naivasha region (see figure 1), created a prominent east–west watershed across this part of the south-sloping rift floor. The appearance of this watershed may have been responsible for the formation of the Lake Naivasha basin to the north.

4. Events at the time of cauldron collapse

4.1. *The caldera*

Collapse of the composite-cone summit region has formed an embayed caldera, *ca.* 7.5 km diameter. Lavas and pyroclastics are exposed in the caldera wall between BJ153944 and BJ160950 (see figures 2 and 3), but elsewhere are completely mantled by syn- and post-caldera pyroclastics. The height of the caldera wall decreases towards the north and east, where it eventually becomes completely buried by the thick succession of later pyroclastics. The form of the pyroclastic-mantled caldera scarp is clearly visible on stereo air photographs, as shown on figure 4, plate 1.

An arcuate ridge, parallel to the caldera wall, protrudes from the base of the young Longonot lava pile between BJ125977 and BJ126960 in the western floor of the caldera (see figures 2–4) and is interpreted as being a possible collapse remnant of the primitive cone structure, mantled by young pyroclastics.

The existence of such a remnant can be used as follows, to define a maximum value for the volume of material consumed during collapse. Assume that (i) arcuate ridge projecting from the base of the younger Longonot lava pile prepresents part of the original summit region of the composite cone; (ii) caldera faults are vertical; (iii) piston collapse has taken place.

Mean radius of caldera = 3.75 km.

Approximate height of missing composite-cone summit above arcuate remnant on caldera floor = 0.6 km.

Maximum volume of material consumed (figure 5) $= \pi \times 3.75^2 \times 0.6$ km^3 = **26.5 km^3**.

4.2. *Syn- and post-caldera pyroclastic activity*

The later stages of caldera collapse were accompanied by pyroclastic flow, base surge, and airfall ash and pumice eruptions, the deposits of which partly infill the caldera depression and mantle the caldera wall and primitive composite-volcano slopes. A decrease in thickness of

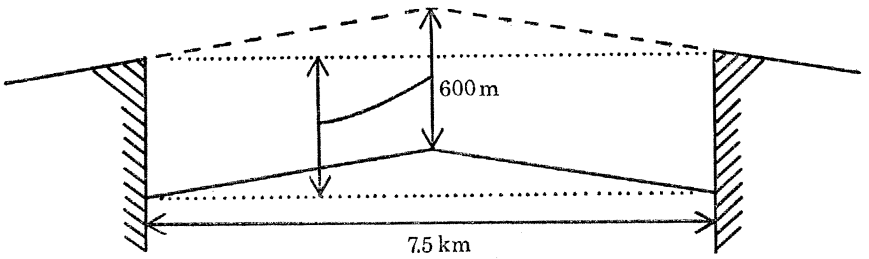

FIGURE 5. Simplified geometry for calculation of the maximum volume of material consumed during caldera collapse.

individual airfall beds away from the caldera demonstrates a source within the caldera depression. The log of borehole C1843 (table 1), situated at BJ105984 on the partly infilled western caldera floor where the exposed beds are all near horizontal, demonstrates that the pyroclastics have a true thickness of 214 m within this part of the caldera depression. At a given distance away from the caldera, the total thickness of pyroclastic cover is always greater to the west; this suggests an easterly wind at the time of eruption of the voluminous airfall component. The airfall component can be traced eastwards to the top of the rift escarpment (G. Goles, personal communication, 1975), but the northern, western and southern limits of the deposit are, at present, uncertain.

Lithological correlation of pyroclastic sections exposed in the walls of the easily accessible gorge between BJ115965 and BJ105940 (see figures 2 and 3) has defined a continuous succession into which isolated exposures at all other localities can be placed (figure 6). As the cumulative exposed thickness is *ca.* 90 m and the lower contact with composite-volcano lavas is not exposed, the recorded succession represents only the upper part of the thick pyroclastic cover. The hump in the correlation profile between sections at BJ109944 and BJ105940 is the result of the pyroclastics being draped over part of the caldera wall that was at a much lower elevation than the surrounding sections.

The exposed succession is subdivided into four lithological units, which, in stratigraphic order are:

Unit IV	predominantly airfall, crystal and vitric ash beds with thin, intercalated, airfall–pumice beds;
Unit III	predominantly airfall–pumice beds with thin, intercalated, ash beds;
Unit II	cross-stratified ash beds, and breccia deposits;
Unit I	block and lapilli tuffs.

4.2.1. *Unit I*

The type section of the Unit I deposits is exposed at BJ107944 and consists of a fractured sequence of non-welded block and lapilli tuffs. The section is summarized in figure 7. Although this is the lowest unit in the exposed succession, it is by no means the earliest deposit of the pyroclastic cover.

The homogeneous, poorly sorted nature of the Unit I beds and the lack of internal stratification suggests emplacement by a rapid succession of pyroclastic flows (Sparks & Walker 1973).

4.2.2. *Unit II*

Several sections in the gorge expose parts of the Unit II succession, but only at one locality, BJ110944, is the entire unit exposed (figure 9*a*, plate 2). The section, summarized in figure 8,

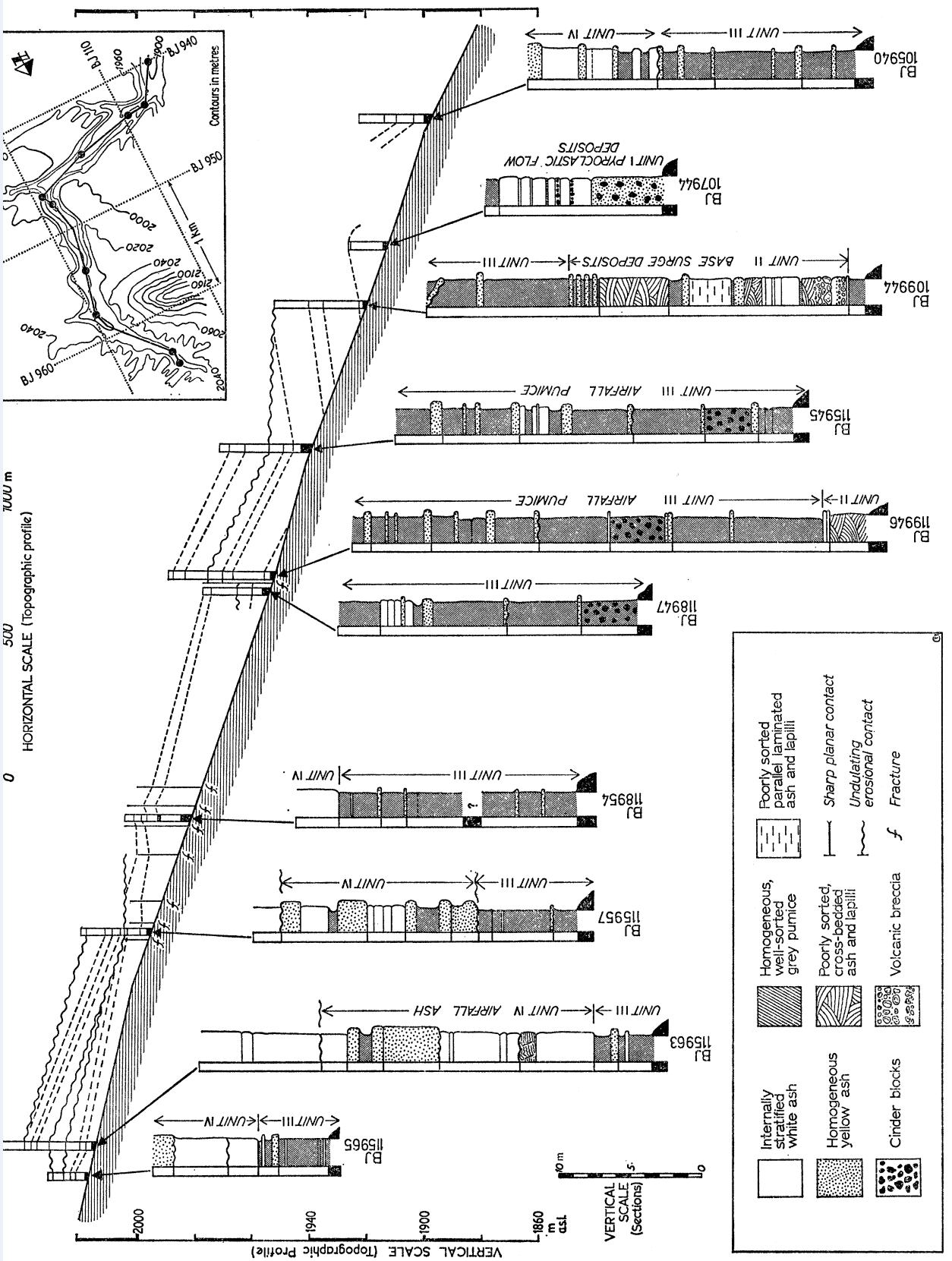

FIGURE 6. Lithological correlation of syn- and post-caldera pyroclastics exposed in the gorge between BJ115965 and BJ105940.

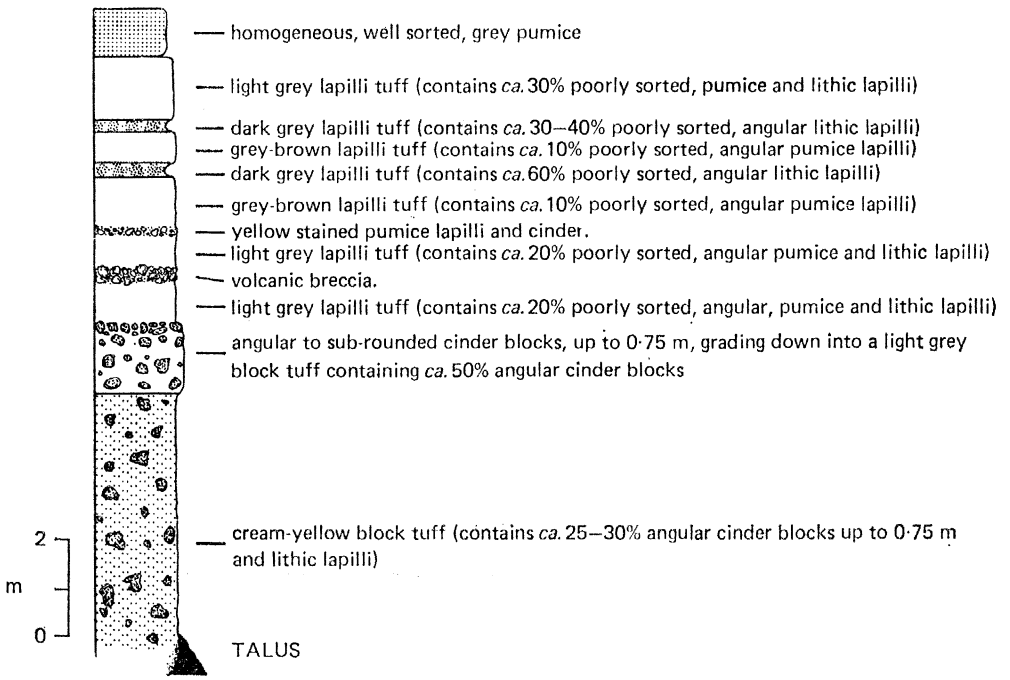

FIGURE 7. Type section of the syn- and post-caldera, Unit I pyroclastic deposits exposed at BJ107944.

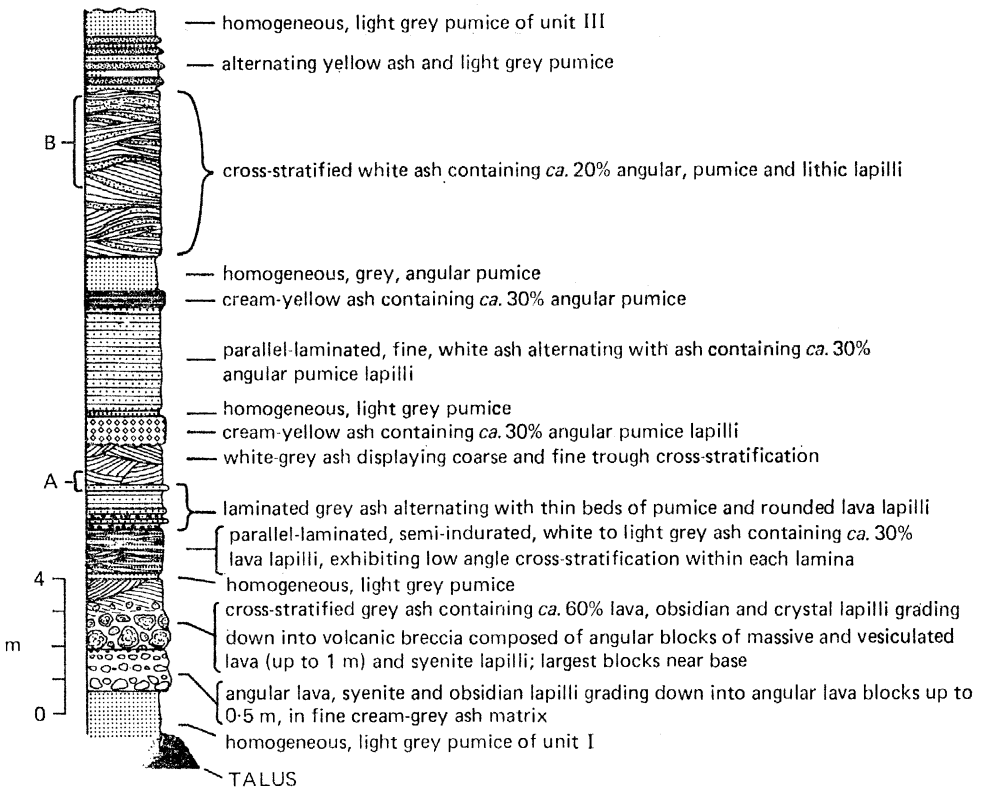

FIGURE 8. Type section of the syn- and post-caldera, Unit II pyroclastic deposits exposed at BJ110944. Sections A, B are parts of the succession shown in figure 9*b*, *c*, respectively.

PHILOSOPHICAL TRANSACTIONS OF THE ROYAL SOCIETY A MATHEMATICAL, PHYSICAL & ENGINEERING SCIENCES

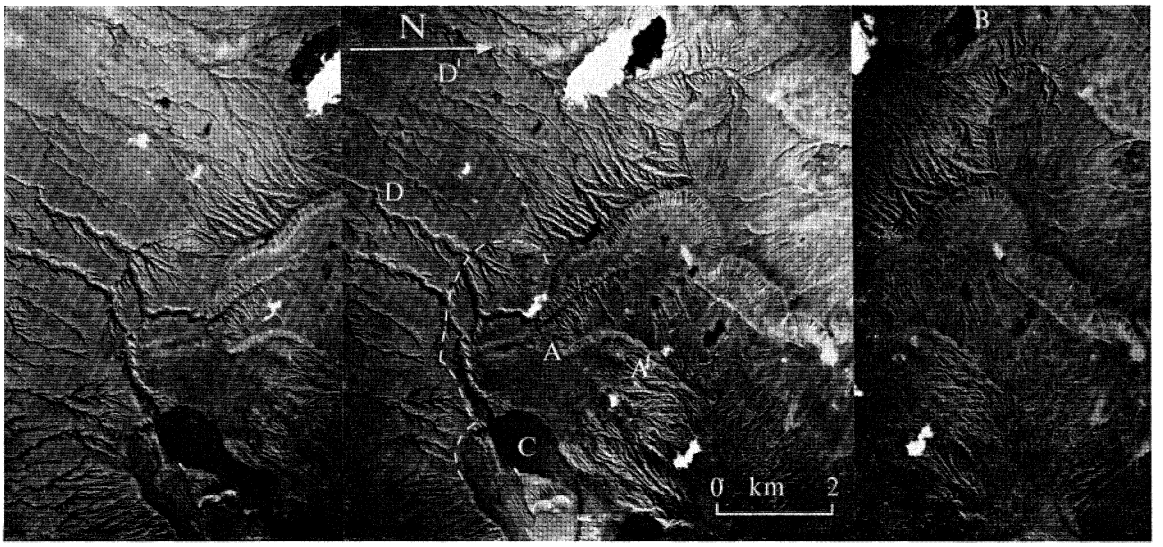

FIGURE 4. Stereo air photographs of the pyroclastic-mantled caldera scarp. Dashed white line indicates the position of the scarp where it is topographically ill defined; A–A′, arcuate, pyroclastic-mantled remnant of collapsed composite-volcano summit region; B, pyroclastic-mantled cone structures; C, recent southwest flank flow; D–D′, linear feature of unknown origin. (Survey of Kenya photographs V13A 1072, 088–090.)

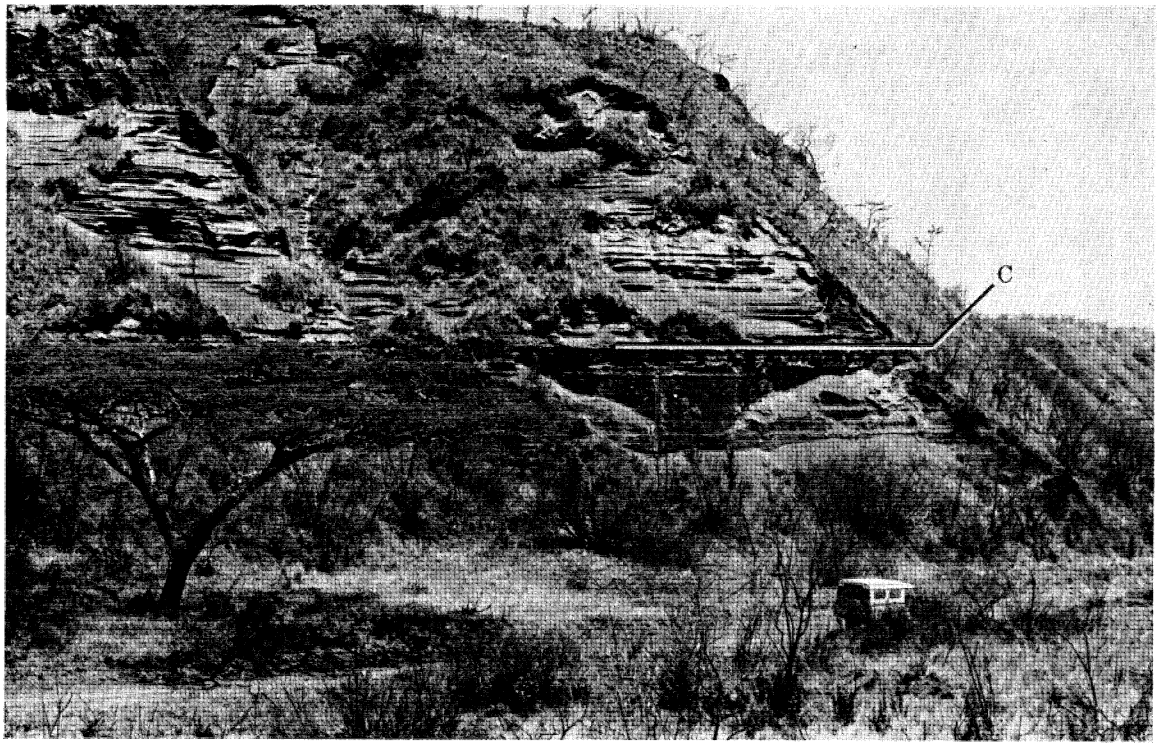

FIGURE 10. Contact, C, between Unit III airfall–pumice beds (below C) and Unit IV airfall–ash beds (above C) exposed at BJ115965. (Landrover at bottom, right, gives scale.)

(*Facing p.* 446)

PHILOSOPHICAL TRANSACTIONS OF THE ROYAL SOCIETY A MATHEMATICAL, PHYSICAL & ENGINEERING SCIENCES

PHILOSOPHICAL TRANSACTIONS OF THE ROYAL SOCIETY A MATHEMATICAL, PHYSICAL & ENGINEERING SCIENCES

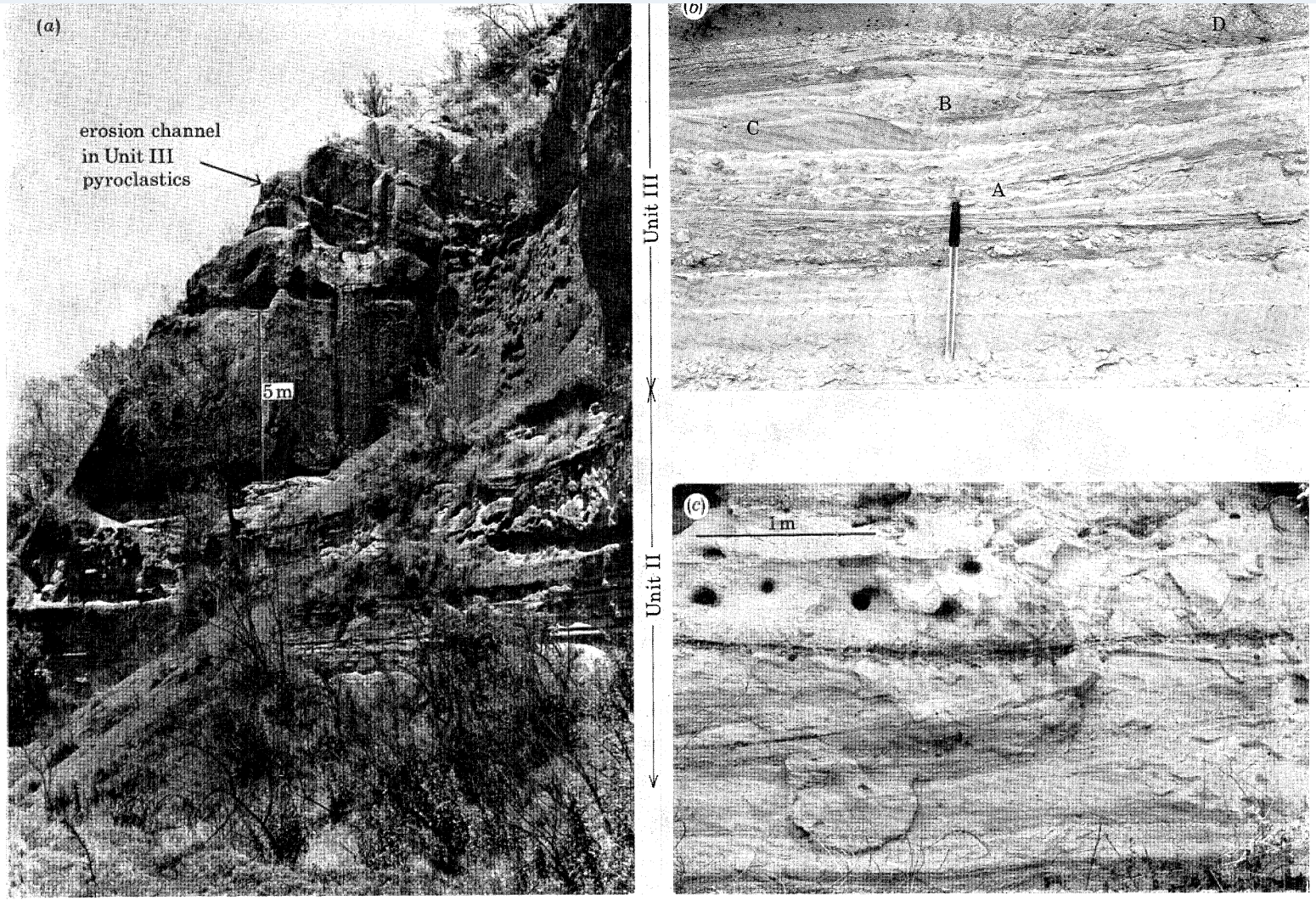

FIGURE 9. (*a*) Type section for the syn- and post-caldera, Unit II pyroclastic deposit exposed at BJ110944. Also visible is the lower part of the overlying Unit III succession which, at this locality, exposes part of an infilled erosion channel.

(*b*) Structures in the base-surge deposit exposed at BJ110944 (see figure 8 for position in type section). A parallel-laminated surge unit is overlain by a unit exhibiting dune cross-bedding. Fine laminations deformed by, and around, larger clasts are seen on the leeside of a dune at A. Possible shute and pool structure at B. Stoss-side slopes, preserved at C and D, are built up from the surface of the lee slope of an underlying dune. Flow is from right to left. Scale: pen length = 15 cm.

(*c*) Structures in base-surge deposit exposed at BJ119946 (see figure 8 for position in type section). Poorly sorted, cross-bedded ash and lapilli horizons are shown in the lower part of the photograph. A poorly sorted, sinuous lapilli horizon with a wavelength of 2.5 m and amplitude of 0.15 m is shown in the upper part of the photograph. Flow is from left to right.

PHILOSOPHICAL TRANSACTIONS OF THE ROYAL SOCIETY A MATHEMATICAL, PHYSICAL & ENGINEERING SCIENCES

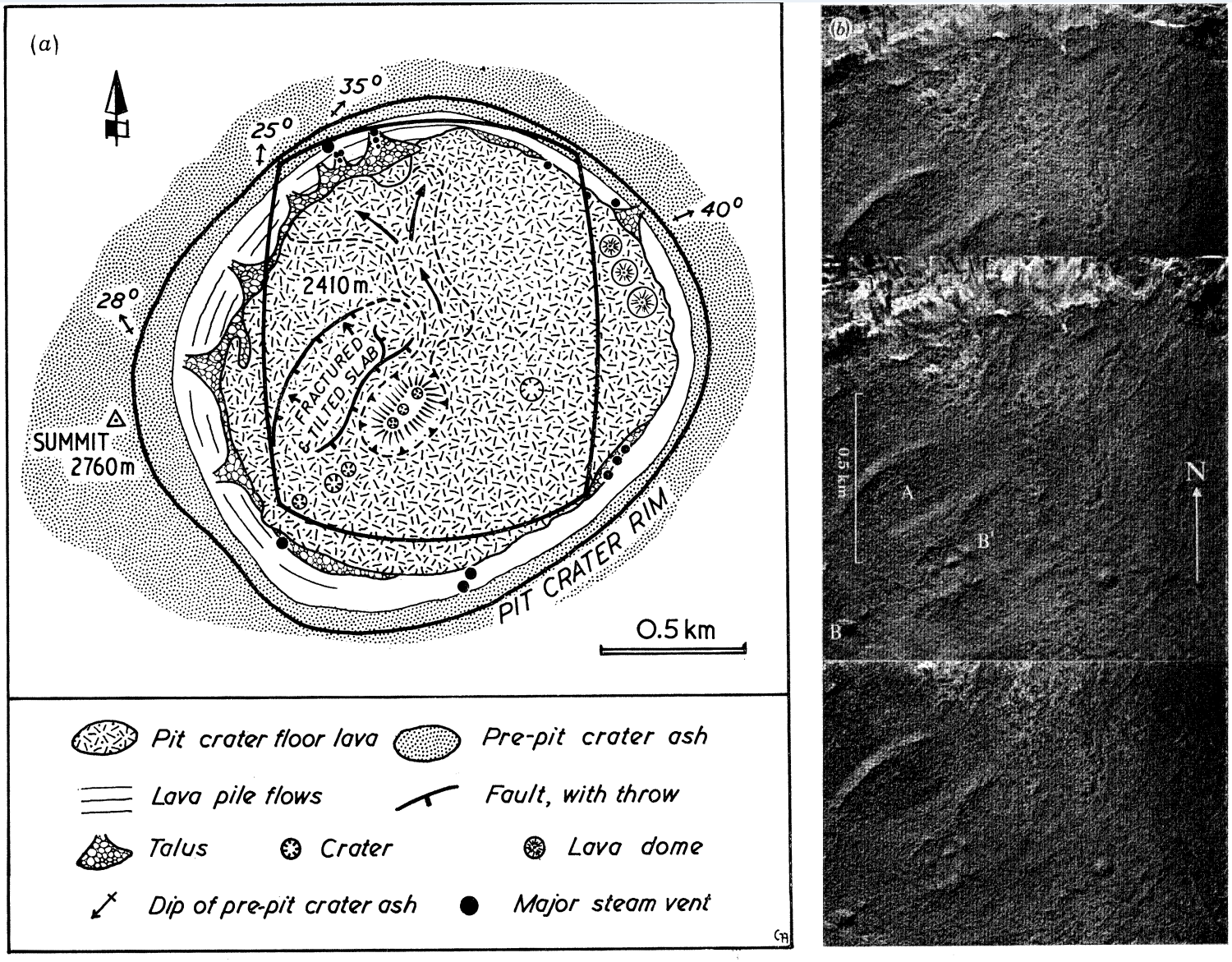

FIGURE 13. (*a*) Photogeological sketch map of the pit-crater floor. (*b*) Stereo air photographs of part of the pit-crater floor delimited by the enclosed area on figure 13*a*. A, fractured and tilted slab; B–B′, crater alignment. (Survey of Kenya photographs 69/90, 153–155.)

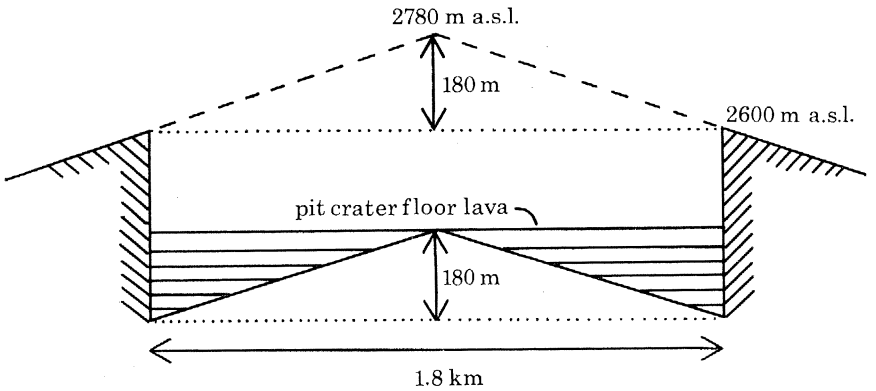

FIGURE 14. Simplified geometry for calculation of the minimum volume of the pit-crater-floor lavas.

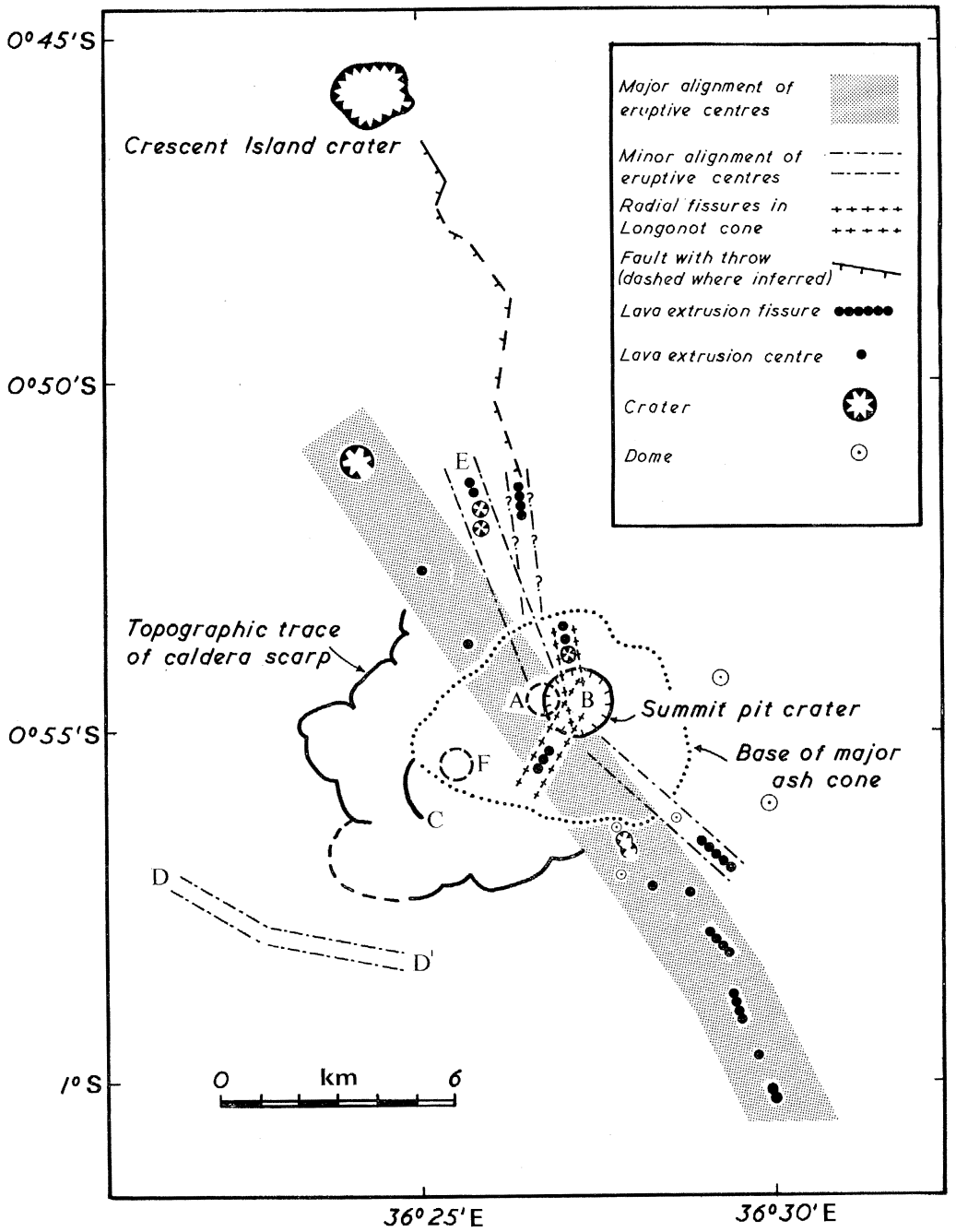

FIGURE 15. Structural sketch map of Longonot volcano. See text for explanation of features labelled A–F.

PHILOSOPHICAL TRANSACTIONS OF THE ROYAL SOCIETY A MATHEMATICAL, PHYSICAL & ENGINEERING SCIENCES

is the type section for the unit. The basal breccia bed has a sharp, undulatory contact with the upper ash and pumice bed of Unit I, owing to indentation of the contact surface by large blocks. Other exposures of parts of the Unit II succession are located at BJ119946, BJ124942, BJ093925 and BJ221967.

Four heterogeneous, cross laminated, crystal–vitric ash beds containing many lithic lapilli occur in the section. These beds cannot be interpreted as primary airfall ash deposits, as such deposits rarely exhibit well developed, dune cross-stratification and are usually well sorted (Sparks & Walker 1973). An origin by flash flooding during heavy rainstorms also seems unlikely as, at BJ125943, preserved sedimentary structures demonstrate deposition from a succession of currents travelling uphill over the caldera wall. According to Sparks & Walker (1973), such features are characteristic of deposits emplaced by a succession of base surges. The surges have low temperatures compared with magmatic temperatures and form during phreato-magmatic eruptions (Waters & Fisher 1970). Details of the structures preserved in two sections cut parallel to the primitive composite volcano slope (i.e. parallel to the flow direction) are shown in figure 9*b*, *c*, plate 2. The structures are very similar to those described from dune cross-bedded, base surge deposits in the Laacher See area of Germany (Schmincke *et al.* 1973) and in the Ubehebe Craters, California (Crowe & Fisher 1973).

The two lower, coarse volcanic breccias are similar to sections of initial vent-clearing breccia, described by Moore (1967), from the deposits of a base surge erupted during the 1965 activity at Taal Volcano, Philippines, while the structure and lithological characteristics of the intercalated pumice beds are identical to those displayed by the Pompeii airfall pumice, deposited during the type Plinian eruption of Vesuvius in A.D. 79 (Lirer *et al.* 1973). The heterogeneous, parallel-laminated, ash and lapilli beds containing lamellae that display large variations in grain size and sorting from one to another are also interpreted as base surge deposits, following Sparks & Walker (1973) and Crowe & Fisher (1973).

To summarize, the Unit II succession is interpreted as an initial, vent-clearing breccia followed by a succession of base-surge deposits produced by eruptions resulting from groundwater repeatedly coming into contact with the magma. Intercalated airfall–pumice deposits were probably derived from violent degassing of the magma after groundwater previously in contact with it had been temporarily cleared during the foregoing base-surge eruptions.

4.2.3. *Units III and IV*

The lack of easily accessible type sections of the complete Unit III and Unit IV successions has made it necessary to define these two units by means of lithological correlation between the numerous accessible sections exposed in the upper part of the gorge.

Unit III consists of an alternating succession of thick, trachytic pumice beds and intercalated, thin, yellow, crystal–vitric ash beds, which mantle underlying topographic irregularities. The pumice beds contain light grey to dark grey coarse, angular to sub-rounded, well sorted, sparsely porphyritic pumice lapilli, generally about 4 cm across, but with some interstitial broken fragments as small as 0.5 cm. Alkali feldspar is the dominant microphenocryst phase found in the pumice lapilli. In the upper part of the gorge at BJ117946, bed thicknesses range from 1 to 4 m. Most beds are very homogeneous, but occasionally a weak stratification occurs, caused by slight changes in colour and size of pumice lapilli. The pumice beds are non-indurated and non-welded, being very loose and crumbly, and, in the sections examined, they do not show much variation of pumice lapilli size with distance from the caldera region, although

PHILOSOPHICAL TRANSACTIONS OF THE ROYAL SOCIETY A MATHEMATICAL, PHYSICAL & ENGINEERING SCIENCES

beds do thin down the composite volcano slope. A prominent bed containing many large, angular cinder blocks decreases in thickness down the gorge, from 4 m at BJ119945 to 2 m at BJ093923, a distance of 4 km. Many beds in the succession contain variable proportions of (i) analcite syenite nodules up to 0.2 m in diameter, in various states of weathering, (ii) crystalline peralkaline trachyte lava lapilli, (iii) sparsely porphyritic, peralkaline trachyte obsidian lapilli and blocks, up to 0.5 m across, displaying distinct flow banding, and (iv) trachyte cinder blocks up to 0.5 m across.

The intercalated ash beds are homogeneous, well sorted and vary from cream–yellow to yellow–brown in colour. The beds are *ca.* 0.3 m thick and have sharp, planar contacts with the underlying and overlying pumice.

Local erosion channels, transgressing into planar erosion surfaces parallel to bedding, demonstrate major periods of quiescence between eruptions, a fine example being illustrated in figure 9*a*. The basal pumice bed of Unit III has a sharp, planar, erosional contact with the uppermost beds of Unit II. Correlation of sections at BJ118954, BJ118947 and BJ119946 show a thickness of 40 m for Unit III in the upper part of the gorge, an estimate that does not include any addition for pumice removed by erosion.

The physical characteristics of the pumice beds rule out an origin by deposition from a sequence of pyroclastic flows (Sparks & Walker 1973), but are identical to those characteristics displayed by the Pompeii airfall–pumice described by Lirer *et al.* (1973). The intercalated, thin, ash beds may represent deposits derived from periodic, weak, vent-clearing activity.

Unit IV is an alternating succession of thick ash beds and intercalated, thin, well sorted, light grey, pumice horizons displaying physical characteristics identical to the airfall pumice of Unit III.

There are four types of ash deposit in the Unit IV succession:

(i) homogeneous, sandy yellow, crystal–vitric ash;
(ii) homogeneous and laminated, fine, grey, crystal–vitric ash;
(iii) homogeneous and laminated, fine, white, crystal ash;
(iv) graded, coarse, black, crystal–vitric–lithic ash.

Bed thickness range from 1 to 4 m. The lower boundary of the unit has a sharp, planar contact with the upper pumice bed of Unit III, as shown in figure 10, plate 1. Correlation of sections at BJ115963 and BJ119957 show that Unit IV has a maximum thickness of 23 m in the upper part of the gorge. The upper Unit IV beds are truncated by a sharp, undulating, erosion surface and overlain by later lava pile flows and pre-pit-crater ash.

The well sorted nature of each bed, the association of these beds with intercalated airfall–pumice beds and the fact that the beds reflect underlying topographic irregularities without significant change in thickness, suggest an airfall origin for the ash.

The change in lithology from Units I to IV records abrupt changes in the style of eruption with time, i.e. pyroclastic flow eruptions → phreatic base-surge eruptions → Plinian, airfall–pumice eruptions → airfall–ash eruptions.

4.2.4. *General considerations*

Within the caldera depression there are many horizons at different levels within the succession, below which the beds have suffered localized fracturing and tilting. Overlying beds mantle the upstanding, fractured and tilted beds and may themselves be included in later

fracturing and tilting at a different locality. Good examples are exposed at BJ107944, BJ120948 and BJ119957. Unit IV is completely unaffected by the fracturing. Outside the caldera depression, pyroclastic units have not suffered such intense fracturing. Such evidence points to late-stage movements of the caldera floor during eruption of Units I, II and III. The unfractured Unit IV, however, was erupted after late-stage, caldera floor movement had ceased.

The airfall component of the pyroclastic succession, being widespread to the west of Longonot, can be employed as a marker horizon within the comendite volcanic succession of southwest Naivasha and is especially useful when comparison is made between the chemical evolution of the volcanic successions erupted in each of these two regions. To the west of the Longonot caldera, the airfall component mantles several underlying, dome-like structures (see figures 3, 4). The most westerly of the structures form an arc, the ground to the west being much flatter and less eroded than that to the east. It is possible that the underlying structures are small lava domes or cinder cones constructed over a ring fault that C. Lamb (personal communication, 1974) suspects to exist in this area.

The syn- and post-caldera pyroclastic cover has a maximum thickness of *ca.* 200 m within the caldera depression. Decrease in thickness is more rapid to the east of the volcano than to the west; this results in an asymmetric, low angle cone form.

On the southwestern slopes of the composite cone, 10 km from the centre of the caldera, the Unit III and Unit IV airfall beds have a thickness of about half that observed near the caldera rim. Further west, exposures of the deposit are limited, as they are covered by later comendite flows from the southwest Naivasha field. If one assumes that the thickness of the airfall component decreases exponentially with distance from the source and that the pyroclastic flow and base surge units remain relatively thick at 10 km from the caldera centre, then a minimum volume for the syn- and post-caldera pyroclastics can be calculated by treating the problem as the volume of a disk with an average thickness of 150 m and a radius of 10 km.

$$\text{Minimum volume of the deposit} = \pi \times 10^2 \times 0.15 \text{ km}^3 = \mathbf{50\ km^3}.$$

For a more accurate estimate of the original volume of the deposit, a detailed, isopachyte map, showing variation in thickness, needs to be constructed. This would involve searching for complete sections of the syn- and post-caldera pyroclastics, especially further west, or trying to identify the unit from the logs of the few boreholes situated west and southwest of the volcano.

4.3. *Cause of caldera collapse*

Johnson (1969) has summarized the mechanisms thought to be responsible for ring-fracture formation and caldera collapse. For Longonot, three possible mechanisms could account for the formation of the caldera:

(i) creation of a void below the magma-chamber roof by withdrawal of magma to deeper levels;
(ii) suction down of the chamber roof by the receding magma;
(iii) rapid evacuation of the chamber as a result of the eruption of late composite-volcano pyroclastics.

The evidence offered by the field relations is insufficient to determine which process is dominant.

After the main collapse event, the continued separation of a gas phase from the liquid resulted in the eruption of the syn- and post-caldera pyroclastic succession. Changes in the

style of eruption recorded by this succession may, in part, reflect a continually falling liquid level in the conduit and feeder system (Rittmann 1962) or a decrease in the quantity of CO_2 in the gas phase (Sparks & Wilson 1978).

5. Lacustrine sedimentation

During the Pleistocene, the level of the lake in the Naivasha basin, to the north of Longonot, fluctuated and was, for a period, higher than the present level. Kamau (1974), studying ancient shoreline features, has identified a maximum lake level of 2000 m a.s.l., 120 m above the present level. Before any further rise could take place, the Hell's Gate overflow channel was cut to the west of Longonot (see figure 3), and the lake level thus reduced to 1940–1950 m a.s.l., where it remained stabilized prior to climatic changes reducing the level again. Using ^{14}C age dates from samples of a Lake Naivasha sediment core, Richardson & Richardson (1972) show that the lake continued to discharge through the Hell's Gate outlet until 5650 a B.P. A second core extracted by Richardson & Richardson from the Lake Naivasha sediments gave ^{14}C age dates for the 2000 m highstand ranging between 12000 a B.P. and 9500 a B.P. (Kamau 1974). Kamau concludes from this that the highstand was not before 12000 a B.P.

On the lower southwestern slopes of the primitive composite volcano, the syn- and post-caldera pyroclastics dip 6° down the lower cone slopes. Near BJ080907, in the southwestern mouth of the easily accessible NE–SW gorge, Unit IV airfall-ash beds continue to dip at 6° under an outwash fan of reworked ash and pumice eroded from the gorge. The same situation prevails at the mouths of other gorges in the area, all aligned down the primitive composite-volcano slope. The fans are related to the local base level of a lake that formed between Suswa and Longonot after Lake Naivasha had overflowed through Hell's Gate gorge (Thompson & Dodson 1963; Kamau 1974); this demonstrates that the age of the pyroclastics is greater than 9500 a.

On the northern Longonot slopes, where deep gullies are absent, Kenya Ministry of Agriculture (Water Development Department) borehole logs, summarized and interpreted in table 1, can also be used to demonstrate that the syn- and post-caldera pyroclastics pre-date the 2000 m Lake Naivasha highstand. Where the upper surface of deposits interpreted to be syn- and post-caldera pyroclastics are below 2000 m a.s.l., they are always overlain by lake sediments. Where the upper surface is at 2000 m a.s.l. or above, the syn- and post-caldera pyroclastics are overlain, not by lake sediments, but by younger pyroclastics.

The lake sediments display a variable lithology consisting of well bedded, diatomaceous silts, of fine ash, and of lava and pumice lapilli.

6. Crescent island crater

Crescent Island, situated in the southeast corner of Lake Naivasha, between BK105167 and BK114146, has a maximum height of 25 m above the 1970 lake level of 1930 m a.s.l. Aerial photographs taken in 1960, when the lake level was 10 m lower, show that the present island is part of the rim of a crater, *ca.* 2 km in diameter. On the steep crater slope at BK110149, a coarse volcanic breccia is exposed, which is composed of angular, accidental blocks of crystalline lava, ranging in size from 2 cm to 3 m across. Mixed hawaiite–peralkaline trachyte lava, vesiculated, light grey, trachyte lava and massive, blue–green, olivine–basalt lava comprise the

TABLE 1. LOGS OF KENYA MINISTRY OF AGRICULTURE (WATER DEVELOPMENT DEPARTMENT) BOREHOLES IN THE LONGONOT AREA

thickness/m	lithology	interpretation
	C210 BK093093 1910 m a.s.l.	
2	soil	soil and lake beds (?)
16	pumice and sand	syn- and post-caldera pyroclastics
4	quartzitic sand with abundant feldspar	
8	buff yellow, sandy clay	
12	highly vesicular lava	composite-volcano lavas and pyroclastics
33	iron-stained sand and agglomerate	
	C567 BK138097 1950 m a.s.l.	
11	light-grey pumiceous lake beds	lake sediments
2	light-grey pumiceous lake beds with lava gravel	
3	light-yellow pumice	syn- and post-caldera pyroclastics
19	light-grey pumice with gravel	
24	green–grey pumice with lava lapilli	
13	obsidian and lava lapilli	
6	fresh, dark-grey, phonolitic trachyte	composite-volcano lavas and pyroclastics
3	fine, mottled, yellow trachyte tuff	
3	fine, grey, mottled ash	
15	light-grey lava gravel	
6	light-grey pumice	
	C729 BK125037 2060 m a.s.l.	
2	fine, light-grey volcanic ash	post-pit-crater ash
21	fine, light-grey volcanic ash, slightly darker and coarser	
8	fawn, earthy ashes containing slightly rounded lapilli	syn- and post-caldera pyroclastics
38	light-grey pumice beds, becoming coarser upwards (?)	
73	yellow to grey ash with lava lapilli	
15	fresh, light grey to dark grey, vesicular trachyte lava	composite-volcano lavas and pyroclastics
8	drab-coloured vesicular lava	
36	light grey and light yellow ash, pumice and lava lapilli	
	C910 BK096082 1930 m a.s.l.	
9	brown–grey lava	mixed lavas
9	lake sediments containing pumice and lava pebbles	lake sediments
6	light-grey pumice beds	syn- and post-caldera pyroclastics
9	grey–brown, coarse and fine lava lapilli with some obsidian chips	
	C1279 BK144070 2005 m a.s.l.	
5	soil	reworked ash and soil
14	fine-grained black–blue vesicular lava	mixed lavas
36	pumice, volcanic ash, volcanic sand and obsidian lapilli	thin covering of lake sediments overlying syn- and post-caldera pyroclastics
50	coarse sand	
55	fine-grained greyish lava	composite-volcano lava
	C1843 BJ105984 2070 m a.s.l.	
214	volcanic ash and pumice	syn- and post-caldera pyroclastics
13	trachyte lava	composite-volcano lavas and pyroclastics
7	fine ash	
30	trachyte lava	
16	volcanic ash and sand	

PHILOSOPHICAL TRANSACTIONS OF THE ROYAL SOCIETY A MATHEMATICAL, PHYSICAL & ENGINEERING SCIENCES

TABLE 1 (*cont.*)

thickness/m	lithology	interpretation
	C1926 BK093054 1980 m a.s.l.	
3	sand and silt	soil and lake sediments
14	coarse pumice	syn- and post-caldera pyroclastics
27	sand in fine-grained deposit	
22	fresh, dark trachyte lava	composite-volcano lavas and pyroclastics
29	heterogeneous, coarse sand	
18	lava	
23	coarse sand in fine matrix	
	C2823 BK201026 2130 m a.s.l.	
92	volcanic ash	syn- and post-caldera pyroclastics
32	hard lava	composite-volcano lavas and pyroclastics
10	yellow tuff	
6	pumice	
3	hard lava	
50	pumice and sand	
147	soft black rock	
	C2997 BJ099999 2170 m a.s.l.	
140	volcanic ash and pumice (with obsidian) and a welded tuff horizon	syn- and post-caldera pyroclastics
65	broken lava with gritty, sandy ash	composite-volcano lavas and pyroclastics
45	volcanic ash and pumice	
23	broken lava with coarse, gritty sand	
67	volcanic ash	

blocks. Apart from this exposure, the whole island is covered by fine, grey ash and by pumice. The position of this pyroclastic cover in the Longonot succession remains unknown.

A core extracted by Richardson & Richardson (1972) from the centre of Crescent Island crater contains lake sediments deposited before 9500 a B.P. The crater must, therefore, have ceased to be active well before this date. It may possibly have been active during the syn- and post-caldera pyroclastic activity.

A normal fault, with a throw of 3 m to the west, can be traced, both in the field and on aerial photographs, from BK128142, near Crescent Island, to BK154052. Between BK128142 and BK133123, the fault scarp exposes a poorly sorted, lapilli tuff containing angular, pumice lapilli up to 2 cm in diameter, angular, lava and obsidian lapilli up to 5 cm and small, alkali feldspar crystals, in a white–cream, ash matrix. Just above the fault scarp, the tuff is overlain by a thin deposit of grey pumice. Although the origin and relations of the lapilli tuff remain unclear, the author suspects that it may be part of the syn- and post-caldera Unit I pyroclastic succession. However, more detailed work is needed to identify its position in the volcanic succession.

7. POST-CALDERA ERUPTIONS

The post-caldera succession is divided into three parts:

(i) an early group of mixed, hawaiite–peralkaline trachyte lavas;
(ii) later, sparsely porphyritic, peralkaline trachyte lavas of the Longonot lava pile;
(iii) terminal, peralkaline trachyte ash and pumice covering the Longonot lava pile and areas to the west, heralding collapse of the summit pit crater.

7.1. *Mixed, hawaiite–peralkaline trachyte lavas*

Eruption of the earliest, mixed, hawaiite–peralkaline trachyte flows onto the northern plains of Longonot took place when the level of the ancient Lake Naivasha had retreated to below 1900 m a.s.l. from its stabilized high-stand at 1950 m. These are hawaiites containing only a small volume of the trachytic liquid component. The early flows were closely followed by eruption of the 'Obsidian Ridge' mixed flow, which almost completely covered the two earlier flows, leaving only their northern extremities exposed. This later, mixed flow became progressively richer in the trachytic liquid component as successive flow units were erupted. The lavas are distinguished in the field by their prominent, rounded clusters of plagioclase feldspar phenocrysts accompanied by phenocrysts of easily recongizable olivine, pyroxene and tabular alkali feldspar. Evidence for mixing of two liquid components can only be observed in thin section. Wispy streaks and lenses of light trachyte occur in the dark, hawaiite matrix of the earlier flows, while, in the later flow units of 'Obisdian Ridge', streaks and lenses of dark hawaiite occur in the lighter, trachyte matrix. Separate plagioclase, augite and forsteritic olivine phenocrysts, characteristic of the hawaiite component, are found scattered through the light trachytic groundmass, although still retaining rims and trials of dark hawaiitic groundmass. Similarly, alkali feldspar, sodic pyroxene and fayalitic olivine phenocrysts, characteristic of the trachytic component, are frequently found scattered through the hawaiite groundmass still retaining rims and trails of the lighter trachytic groundmass. Details of the petrography and chemistry of these lavas are to be discussed in a later publication.

The northern extremities of the two earlier flows are veneered by a thin, brown soil, developed on reworked ash. Hillocks, up to 4 m high, composed of many dark grey, vesiculated, porphyritic lava blocks, protrude through the covering, permitting sampling of the flow, and are interpreted as being ramp structures. The flow margins were delineated by following a prominent break in slope, which enclosed all the exposures of lava hillocks.

The northern area of the 'Obsidian Ridge' flow is well exposed, having only a thin cover of reworked ash, but towards the south and southeast the flow becomes progressively covered by an increasing thickness of such ash. In the southwest, reworked ash has completely covered the flow surface, leaving only isolated lava hillocks, up to 8 m high, protruding. The surface of the northern area displays many crescent-shaped drag folds, pressure ridges and isolated lava hillocks, which have a thin crust of dense, black, volcanic glass, covering vesiculated porphyritic glass and grading into a dense, light grey, crystalline interior. The source of the 'Obsidian Ridge' flow is located at BK140050.

An idea of flow thickness is obtained from borehole logs. The log of borehole C1279 (table 1) demonstrates a thickness of 14 m near the margin of the 'Obsidian Ridge' flow (or Obsidian Ridge plus earlier flows) at BK144070 while that of borehole C910 (table 1) demonstrates a thickness of 9 m for the earlier mixed flow at BK095083. An incomplete section through the southern part of the 'Obsidian Ridge' flow is exposed in the western wall of the crater at BK143044 and shows that the flow surface dips south, possibly into the partly infilled caldera depression.

Borehole log C910 (table 1) indicates that the earliest mixed flow overlies lake sediments. As the flow surface is covered by a thin veneer of reworked ash and no exposures of lake sediments were observed, the flow must have been erupted after the lake level had returned below the level of the flow margin.

PHILOSOPHICAL TRANSACTIONS OF THE ROYAL SOCIETY A MATHEMATICAL, PHYSICAL & ENGINEERING SCIENCES

The volume of the northern plain lavas is calculated as follows:

average thickness = 20 m;
approximate original aerial extent = 25 km^2;
therefore, volume = **0.5 km^3**.

7.2. *The Longonot lava pile*

Repeated eruption of sparsely porphyritic to aphyric, peralkaline trachyte lava from a major centre on the infilled eastern caldera floor formed a small lava shield, 550 m high and *ca.* 10 km in diameter. Lava also issued from minor centres on the flanks of the growing shield.

The summit region of the shield has been consumed during later pit-crater collapse. Sections through the youngest lavas exposed in the pit-crater wall show no evidence of intercalated pyroclastic horizons. Change in dip orientation of individual lava flows traced around the pit-crater wall demonstrates that the youngest lava-pile flows issued from a source region situated around BJ162990 and that the lava pile had a broad, low-angled summit region.

Lava-pile flows in the west have been completely buried by younger ash deposits, but, in the north, east and south, only the surfaces of flows have been covered; individual flow margins have been left exposed. The earliest flows overlie eroded syn- and post-caldera pyroclastics at BJ119950, BJ217954 and BJ220968, while at BK151043 an early lava-pile flow overlies the southern limit of northern plain, mixed lava. The latter relation demonstrates that the lava-pile flows post-date the northern plain, mixed lavas.

The lavas are characterized in the field by a scattering of tabular, glassy, alkali feldspar phenocrysts and ferromagnesian microphenocrysts, set in a dark-grey groundmass often showing the development of a platy flow cleavage. Two flows, one around BJ212945 and the other around BK182012, contain abundant, angular xenoliths of purple, plagioclase-augite-magnetite-phyric basic lava.

The relative age of every individual lava-pile flow cannot be completely deduced by means of physical correlation alone. In many small sectors of the shield, flows are piled one on top of the other, so that their relative ages may easily be deduced. Correlation of all the flows in one sector with those in another is, however, difficult, owing to a lack of common marker flows and the fact that exposed parts of flows in one sector commonly abut directly against the exposed parts of flows in another sector, with no indication of relative age. Some flows, such as those at BK130030 and BK154046, are completely isolated from the lava pile, although are known to be of lava-pile age. The use of regular variations in whole rock, trace element concentrations proves to be the only method of establishing the relative age of every exposed lava pile flow. The method will be described in a later paper dealing with the chemistry of the centre.

In any one sector of the shield, the morphology and physical properties of flows change consistently with increasing height in the lava pile (i.e. decreasing age) as follows:

(i) the thickness of flows increases from less than 9 m to 30 m;
(ii) flows become progressively shorter in length and take on a rounded, bulbous outline;
(iii) the size and concentration of vesicles progressively decrease, the youngest flows displaying massive, non-vesiculated interiors;
(iv) the modal percentage of phenocrysts decreases from 8 to 0%.

The coalescing of flows repeatedly erupted from five, closely spaced, flank centres aligned along a NE–SW fissure has produced an elongate, lava tableland in the southwest of the

region. The northern tableland flows have a covering of pre-pit-crater ash and, at BJ209926, overlie one of the early lava-pile flows, thus demonstrating their lava-pile age. In addition, contemporaneous flank activity produced peralkaline trachyte lava flows around BK127026 and BK153048, endogenous domes at BJ179946 and BJ178958, and exogenous domes at BK206001 and BK218965. Flank flows range in thickness from 10 to 30 m and have never travelled more than 2 km from their source.

The volume of the lava pile is calculated, with the assumption that its shape approximates to a low-angle cone:

average radius of lava pile base = 5 km;
height of pile = 550 m;
volume of lava pile = $\frac{1}{3} \times \pi \times 5^2 \times 0.55$ km^3 = 15 km^3;
flank eruptions account for *ca.* 1 km^3;
therefore, total volume of lava pile eruptives = **16 km^3**.

7.3. *Pre-pit-crater ash eruptions*

The growth of the Longonot lava pile was terminated by a phase of explosive activity, which produced a thick, ash covering on the broad summit region of the lava pile, and a thinner covering elsewhere.

The thick, summit ash accumulation, along with the lava-pile summit, has been partly consumed during the subsequent pit-crater collapse. A pre-pit crater age is demonstrated by the ash beds around the pit-crater rim, which dip 25–40° down the slope of the lava pile and are abruptly truncated, along with lava-pile flows, at the pit-crater wall. Dip directions and thickening of the truncated ash beds define an eruptive centre around BJ161992, just east of the present Longonot summit and corresponding in position to the younger lava-pile eruptive centre. At a given distance away from the vent, the ash deposit is always thicker to the west of the lava pile, suggesting either an easterly wind at the time of eruption or a vent angled towards the west. The former appears more likely, in view of the easterly winds that prevail at present.

A section through the easily accessible lower part of the ash succession preserved in the pit-crater wall is summarized in figure 11 and shows deposits from the initial vent-clearing eruptions. A description of the complete ash succession recorded in the upper pit-crater wall was unobtainable owing to the loose and precipitous nature of the succession. The thick ash covering has been deeply dissected, especially in the west, exposing ash sections that display numerous small erosion troughs, cut at different levels in the succession and infilled by later ash beds that reflect the underlying topographic irregularities. Such structures demonstrate distinct periods of quiescence between eruptions. On the lower slopes, reworked ash, eroded during such periods of quiescence, is preserved as thin beds displaying small-scale cross laminations.

Intercalated with the ash beds are thin, well sorted, homogeneous, light grey pumice beds containing thin horizons of obsidian lapilli. The good sorting, the mantle bedding and the steep cone form displayed by the ash and intercalated pumice beds point to an airfall origin (Sparks & Walker 1973).

Within the southern part of the area covered by the mixed flows, there are two prominent craters, one at BK113055 and the other at BK143044, and a steep-sided cinder cone at BK143038. Mixed, hawaiite-peralkaline trachyte lava blocks constitute a major component of the volcanic breccia associated with these structures, demonstrating that the two craters and the cinder cone post-date the mixed lavas. A thin veneer of pre-pit-crater ash, combined with the

PHILOSOPHICAL TRANSACTIONS OF THE ROYAL SOCIETY A MATHEMATICAL, PHYSICAL & ENGINEERING SCIENCES

explosive nature of the activity that formed these structures, suggests that they were active during the eruption of the pre-pit crater ash cover.

Like the syn- and post-caldera pyroclastics, the widespread pre-pit-crater ash unit can be employed as a marker horizon within the comendite volcanic succession of southwest Naivasha. Although lithologically similar to many of the comendite ashes, the unit can still be distinguished by its contrasting major oxide chemistry and its unique trace element ratios.

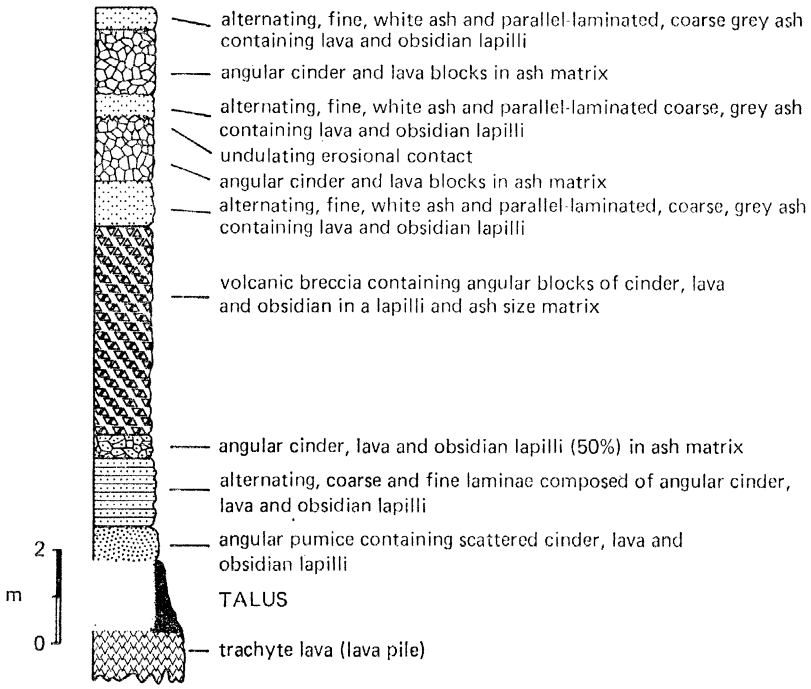

FIGURE 11. Section of lower pre-pit-crater ash deposits exposed in the pit-crater wall at BK173001.

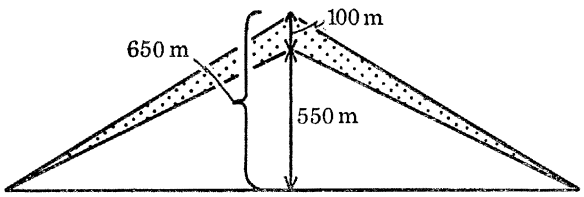

FIGURE 12. Simplified geometry for calculation of the minimum volume of the pre-pit-crater ash.

For the volume of ash erupted, the ash cone is assumed to represent a uniform capping on the lava pile, thickening towards the summit (figure 12).

$$\text{Minimum volume} = (\tfrac{1}{3} \times \pi \times 5^2 \times 0.65) - 15 \text{ km}^3 = \mathbf{2\ km^3}.$$

This configuration is an oversimplification of the real case, as the ash covering is asymmetric in shape, being thicker to the west than to the east, and extends westwards beyond the base of the lava pile. Once again, a detailed isopachyte map would have to be constructed in order to improve the accuracy of the calculation. A thin veneer of this deposit, covering a large area, could add significantly to its volume. The above calculation, however, serves as a good first approximation.

8. Pit-crater collapse

The second major collapse at Longonot produced a circular pit crater, 1.8 km in diameter, at the summit of the lava pile.

The centre of the pit crater lies 0.5 km east of the original lava-pile and ash-cover eruptive centre. Consequently, the depth of the crater between the flat, lava-covered floor and the rim varies from 340 m in the west, below the present Longonot summit, to 80 m in the east. The form of the crater and its asymmetric position with respect to the original summit vent suggest that subsidence has taken place along a circular ring fault of small diameter, rather than by peripheral collapse into the original summit vent.

As there are no collapsed remnants of the lava-pile summit region, only a minimum volume of material consumed during collapse can be calculated, with the assumptions that:

(i) the summit collapses as one body;

(ii) the pit-crater-floor lavas just cover any remnant of the collapsed lava pile and ash cone;

(iii) the lava-pile summit region was originally located over the centre of the pit crater collapse and not over its western margin. This assumption only slightly increases the true value of the minimum volume.

Radius of pit crater = 0.9 km.
Height of original summit above pit crater floor = 370 m.
Minimum volume of material consumed = $\pi \times 0.9^2 \times 0.37$ km^3 = **0.94 km^3**.

Emptying of an underlying magma reservoir during the pre-pit-crater ash activity may have been the cause of the pit-crater collapse.

9. Post-pit-crater eruptions

The post-pit-crater succession is divided into two parts:

(i) mixed, hawaiite–peralkaline trachyte lavas erupted onto the pit-crater floor;

(ii) recent peralkaline trachyte lavas erupted from radial fissures on the southwestern and northern lava-pile slopes.

9.1. *Pit-Crater-floor lavas*

Following collapse, the pit crater was partially infilled by mixed, hawaiite–peralkaline trachyte 'aa' lava, lithologically similar to that erupted earlier on the northern plains. Blocks of the mixed lava, up to 1.5 m across, rest on eroded ash around the pit-crater rim and upper lava-pile slopes, demonstrating that strong explosive activity accompanied, or just post-dated the eruption of these lavas.

A dense growth of thick scrub and trees covering the lavas necessitated the use of photo-geological interpretation to map volcanic features on the pit-crater floor (see figures 13*a*, *b*, plate 3). A prominent line of small craters, extending from the southwest pit-crater wall at BJ163985 to the centre of the crater, defines a radial fissure (figure 13*a*). To the northwest of this crater line, a slab of lava, 0.5 by 0.25 km, is tilted away from the alignment of craters. A flow erupted from the northeast extremity of the crater line has, in part, been guided by the steep southeast wall of the tilted lava slab, and thus post-dates tilting. These features suggest

slight late-stage resurgence of the western pit-crater floor from below the general area of the crater line.

The minimum volume of mixed lava flooding the pit crater is calculated, with the assumption that:

(i) average height of crater rim = 2600 m;
(ii) the lavas just cover a uniformly collapsed lava-pile summit;
(iii) the summit region was originally located over the centre of the pit-crater collapse.

Radius of crater = 0.9 km.

Minimum depth of lava at crater walls (approximate altitude of original summit − average altitude of crater rim) = 2780 − 2600 m = 180 m.

Minimum volume (figure 14, plate 4) = $\frac{2}{3} \times \pi \times 0.9^2 \times 0.18$ km^3 = **0.339 km^3**.

9.2. *Flank eruptions*

9.2.1. *The southwestern flank flow*

On the southwestern slopes of the lava pile, a compound peralkaline trachyte flow, containing sparse microphenocrysts of alkali feldspar, pyroxene and olivine and formed of four flow units, was erupted from a line of six small craters that form a southwestern extension of the crater alignment identified on the pit-crater floor. The complete alignment delimits a radial fissure centred on the pit-crater collapse.

The cooling unit is 4.25 km long, is 1 km at its widest and has an average marginal thickness of 8 m. On the higher slopes, flow units are initially confined to pre-existing erosion gullies cut into the pre-pit-crater ash; this results in widths of less than 0.25 km. Where the gradient eases onto the flat, ash-covered surface of the most southwesterly lava-pile flow, the flow units spread out to become much wider. Between BJ138948 and BJ147952, flow Unit IV poured over the margin of this lava-pile flow to become confined by a narrow gully, which it followed westwards before splitting into two off-shoots, each confined by a gully on opposite sides of a spur in the mantled caldera wall.

The earliest flow unit, Unit I, has a non-fractured, vesiculated, glassy crust with drag folds and a scattering of glassy blocks derived from broken folds. The vesiculated, glassy crusts of Units II and III also display drag folds, but here the crust has been broken into large, tilted slabs and pressure ridges. Flow Unit IV displays a typical 'aa' flow surface. Indirect evidence from the thickness of vegetation cover and youthful surface morphlogy suggests that the southwestern flank flow is very recent indeed, probably 200–300 years old, and post-dates the eruption of the pit-crater-floor lavas.

The late-stage resurgence on the southwestern pit-crater floor below the general area of a radial fissure may be associated with the eruption of the southwestern flank flow from lower down the same fissure line. If so, the pit-crater-floor flow erupted from the northern extremity of the fissure may be trachytic in composition.

9.2.2. *The northern flank flow*

On the northern slopes of the lava pile a peralkaline trachyte flow containing sparse microphenocrysts of alkali feldspar, pyroxene and olivine was erupted from the northern extremity of a radial fissure centred on the pit-crater collapse. The fissure is delimited between BK165006 and BK165012 by the alignment of a collapsed, exogenous lava dome, two small breccia cones and a large cinder and breccia parasitic cone.

PHILOSOPHICAL TRANSACTIONS OF THE ROYAL SOCIETY A MATHEMATICAL, PHYSICAL & ENGINEERING SCIENCES

The flow is composed of four flow units, is 2.5 km long and has an average marginal thickness of 10 m. Flow unit I has a non-fractured, vesiculated, glassy crust with small drag folds and surface blisters up to 2.5 m across, and merges into the eastern slope of the collapsed dome at BK166012, with which it appears to be contemporaneous or which it pre-dates. Unit II has a pahoehoe surface broken into large tilted slabs and pressure ridges. Unit III, erupted, from a source on high ground at BK162016, has a rubbly 'aa' surface consisting of angular crystalline and scoriaceous blocks up to 5 m across. Rubbly lava levées near the source have channelled lava northwestwards into the main body of the unit that was spreading over the lower lava-pile slopes. Unit IV is also of a 'aa' type and was erupted from a source at BK165012, in a gorge formed where the northern side of the collapsed lava dome has been partly removed. Blocks, up to 15 m across and composed of successions of thin lava units identical to the internal structure of the collapsed lava dome, are found on the surface of the unit, at BK162014, where they are banked up against the margin of Unit III. This suggests that the eruption of Unit IV caused the collapse and removal of the missing section of the dome.

The northern and southwestern flank flows both display the same change in surface morphology, from pahoehoe to 'aa', with the eruption of successive flow units. Indirect evidence from the thickness of vegetation cover and youthfulness of morphology suggests that the eruption of the northern flank flow post-dated the eruption of the pit-crater-floor lavas, but was approximately contemporaneous with the eruption of the southwestern flank flow.

The volume of the southwestern and northern flank flows is calculated as follows:

average thickness = 10 m;
approximate area covered = 4.5 km^2;
therefore, volume = **0.045 km^3**.

Present activity is confined to the release of steam from fumaroles around the base of the pit crater wall. Location of major steam vents in March 1974 are shown on figure 13*a*.

10. Structure

The structure of the area covered by Longonot volcano is summarized in figure 15. The main features are:

(i) A major NW–SE alignment of 14 eruptive centres, which includes the source region of the younger lava-pile flows, situated approximately mid-way and indicated by the broken circle at A. This alignment is parallel to the general trend of the rift wall faults between Naivasha and Nakuru.

(ii) Two minor alignments of centres, which, when projected towards the lava pile, pass through the source region at A. All the centres except E, from which the mixed lavas of 'Obsidian Ridge' were erupted, were active during the lava-pile period. A third major alignment is marked on figure 15, plate 4, but is conjectural, as it is defined by only one elongate lava fissure of lava-pile age. Remaining centres are isolated to the east of Longonot.

(iii) Two radial fissures centred on the pit-crater collapse at B. Both fissures were active after pit-crater collapse.

(iv) Minor structural features: a possible collapsed remnant of the composite volcano at C; a photogeologically identified, linear feature in the post-caldera pyroclastics between D and D′, caused by a slight hump in the pyroclastic beds reflecting an unidentified, underlying, linear

body (see also figure 4); a normal fault, post-2000 m lake highstand, with a minimum throw of 3 m to the west, extending from Crescent Island to the base of the lava pile.

(v) An eastward migration of the centre of activity from the composite-volcano summit region situated approximately at F, through the lava-pile and ash-cover source region at A to the pit-crater centre at B.

The structural features outlined above suggest that the locations of the main eruptive centres were essentially controlled by a NW–SE fissure zone, perhaps linked in some way to rift faulting. The alignment of centres of lava-pile age, situated east of the major alignment, has been controlled by local fissures radiating from the main lava-pile and ash-cover source at A. All the exposed centres active during the lava-pile and ash-cover periods are either within the major alignment of centres or are scattered to the east of it. No centres of lava-pile or ash-cover age are visible west of the major alignment. The eastward migration of activity with time may be related to cross faulting on the rift floor.

The preserved section of the caldera wall is entirely confined to the west of the NW–SW alignment of centres. This, however, is a result of a decrease in the absolute height of the rim towards the north and east, where it becomes obscured by voluminous post-caldera pyroclastic deposits and lava-pile flows.

11. Discussion

11.1. *Volume relations*

The original volume of volcanic products is given in tables 2A and 2B.

Table 2A. Original volumes of volcanic products erupted during each episode of activity and their equivalent liquid volumes

eruptive unit	volume of volcanic product/km³	dense rock equivalent volume/km³	liquid equivalent volume/km³
composite volcano	280.0 trachyte lava 140†	140	147
	280.0 pyroclastics 140†	28[1], 42[2], 56[3]	29.4[1], 44.1[2], 58.8[3]
syn- and post-caldera pyroclastics	50.0‡	10[1], 15[2], 20[3]‡	10.5[1], 15.75[2], 21‡
mixed lavas, northern plain	0.5	0.5	0.525
lava-pile flows	16.0	16.0	16.8
ash cone	2.0‡	0.4[1], 0.6[2], 0.8[3]‡	0.42[1], 0.63[2], 0.84[3]‡
mixed lavas, pit crater	0.34‡	0.34‡	0.357‡
post-pit-crater trachytes	0.045	0.045	0.047

† Boreholes C1843, C2997 and C2823, which penetrate the composite-volcano structure, suggest that the ratio of lava to pyroclastics is approximately 1:1.

‡ Minimum values.

1, 2, 3: Assuming (1) 80 %, (2) 70 %, (3) 60 % vesicles, packing voids and non-magmatic ejecta in the pyroclastics.

The volumes of vesicles and of xenoliths present in the lavas are small compared with the total volume of solid lava, so that the values for the original volumes can be taken to be dense rock volumes. Equivalent liquid volumes are about 5 % greater (G. P. L. Walker, personal communication, 1978), owing to loss of volatiles during eruption and to contraction of the rock body during crystallization.

TABLE 2B. ORIGINAL VOLUME OCCUPIED BY EACH TYPE OF VOLCANIC PRODUCT AND THEIR EQUIVALENT LIQUID VOLUMES

volcanic product	volume of volcanic product/km³	dense rock equivalent volume/km³	liquid equivalent volume/km³
trachyte lava	156.05	156.05	163.85
mixed lavas	0.84	0.84	0.882
pyroclastics	192.0†	38.1[1]; 57.6[2]; 76.8[3]†	40.3[1]; 60.48[2]; 80.64[3]†

† Minimum values.
1, 2, 3: Assuming (1) 80 %, (2) 70 %, (3) 60 % vesicles, packing voids and non-magnetic ejecta in the pyroclastics.

The pyroclastic deposits contain much accessory and accidental ejecta, the volume of which must be subtracted from the total to give the volume of essential magmatic ejecta. The essential ejecta, moreover, are often loosely packed and retain their original vesicularity, so that the dense-rock equivalent volume, and hence the liquid equivalent volume, is less. The liquid equivalent volumes for the pyroclastics have been calculated with use of the assumption that between 60 and 80 % of the volume of pyroclastics are non-magmatic. These values are based on dense-rock equivalent volume calculations on the Granadilla Pumice deposit, Tenerife (Booth 1973), the Pompeii Pumice, Vesuvius (Lirer *et al.* 1973) and the Granadilla ignimbrite (Booth 1973). Once again, liquid equivalent volumes are about 5 % greater.

The volume data presented in tables 2A and 2B have three important consequences in relation to the collection of a sample suite representative of the volumes of liquid erupted.

(1) At a minimum, *ca.* 20 % of the total volume of liquid erupted at Longonot has been erupted as pyroclasts. For an ideal sample suite representative of the volumes of liquid erupted, at least 20 % of the samples should be pyroclastic. To sample pyroclastics for chemical analysis presents its own special problems, however, because ash and pumice are very susceptible to significant change of the overall chemistry by secondary alteration. Since a large proportion of the total sample suite is involved, a very careful and critical approach to sampling is required to collect unaltered, pristine samples representing the nearest possible approach to the true pyroclastic liquid composition.

(2) Products formed from the greater part of the total volume of liquid erupted at Longonot are not exposed. This creates a serious sampling problem if the scheme is to be representative of the volumes of liquid erupted during the entire volcanic history of the centre. A sample suite truly representative of liquid volumes erupted during specific periods of activity can only be collected from products erupted during and after the upper syn- and post-caldera pyroclastic activity. The remaining products, which represent the greater part of the total volume of liquid erupted, cannot be directly sampled. Indirect sampling from borehole cores or lava nodules could partly alleviate the undersampling problem, but, as Walker (1973) points out, both of these sampling methods generally give a biassed sample suite unrepresentative of the erupted liquid volumes. Either way, the sample scheme will be unrepresentative of liquid volumes erupted over a period covering the entire history of the volcano. Only a very small part of the total liquid volume can be adequately sampled along the lines suggested by Walker.

(3) Although the mixed, hawaiite–peralkaline trachyte lavas account for less than 1 km³ of liquid, they are critical to the understanding of the origin of the trachyte melt at Longonot as they represent the only evidence for coeval basic and felsic magmas. Thus, despite their small

PHILOSOPHICAL TRANSACTIONS OF THE ROYAL SOCIETY A MATHEMATICAL, PHYSICAL & ENGINEERING SCIENCES

volume, the mixed lavas deserve very detailed petrographic and chemical study, even to the extent of being oversampled relative to the rest of the succession. Provided that one realizes and accepts that the mixed lavas are purposely oversampled, these can be accommodated into the sample suite without fear of upsetting any later petrogenetic interpretations.

From the data presented in table 2A, it is very difficult to assess the volumetric relations between the major collapse structures and their possible associated eruptives. A minimum liquid equivalent volume of 0.84 km³ for the pre-pit-crater ash cover, based on an assumption of 60% non-magmatic material and voids, is very close to the minimum volume of material consumed during pit-crater collapse, i.e. 0.94 km³. However, it is stretching the argument to suggest that the liquid volume equivalent to the ash-cover eruptives is equal to the volume of material consumed during pit-crater collapse, especially when comparing minimum volumes. Similarly, the liquid volume data for the late composite-cone eruptives and the syn- and post-caldera pyroclastics is not sufficiently accurate to allow any meaningful comparisons with the volume of material consumed during caldera collapse.

11.2. *Comparison with the nearby Quaternary caldera volcanoes, Menengai and Suswa*

In addition to Longonot there are two other caldera volcanoes in the Quaternary Nakuru–Naivasha peralkaline province; the peralkaline trachyte volcano, Menengai, 80 km to the north, and the sodalite trachyte and peralkaline phonolite volcano, Suswa, 15 km to the south (figure 1). As all three centres were active during the same period, a comparison of their volcanic histories is useful for establishing any overall similarities in their eruptive styles.

In table 3 the volcanic histories of the three centres are compared; the following facts emerge:

(i) Longonot is the only centre to show a pre-caldera succession of pyroclastics as well as lavas, although Menengai does display a trachytic ignimbrite at the top of its pre-caldera lava succession.

(ii) The first collapse event at Menengai and Suswa produced calderas elongated along ENE axes. Although the first caldera at Longonot is partially buried by later eruptives, it too appears to have an ENE axis, but one measuring only 7.5 km, in contrast to the 11–12 km of the other two.

(iii) Explosive activity has accompanied caldera collapse at all three centres.

(iv) A similar state of erosion of syn-caldera pyroclastics suggests that the Suswa caldera may be coeval with that at Longonot. That of Menengai is *ca.* 10000 years old (McCall 1967), this being very close to the minimum age of the syn- and post-caldera pyroclastics on Longonot; this suggests that the three calderas may be of essentially similar age. If so, a regional episode of caldera formation may have taken place.

(v) At Longonot and Suswa, the post-caldera eruptives have constructed secondary lava volcanoes on the infilled caldera floors. At both volcanoes, the summits of the secondary lava volcanoes have collapsed to form pit craters; these have diameters of 1.6 and 1.8 km at Suswa and at Longonot, respectively. Suswa demonstrates a third major collapse feature, the annular ring graben, formed after pit-crater collapse.

(vi) Recent flows, 100–300 years old, have been erupted at all three centres.

(vii) Longonot is the only volcano on which mixed basic–felsic lavas have been identified. These lavas were the first extrusive products erupted after each major collapse event.

(viii) Activity at Longonot was initiated at approximately the same time as that at Suswa, *ca.* 400000 years B.P. Although the early Menengai volcano is in a similar state of preservation

PHILOSOPHICAL TRANSACTIONS OF THE ROYAL SOCIETY A MATHEMATICAL, PHYSICAL & ENGINEERING SCIENCES

TABLE 3. COMPARISON OF THE VOLCANIC HISTORIES OF THE QUATERNARY CALDERA VOLCANOES MENENGAI, SUSWA AND LONGONOT

volcano	pre-Caldera eruptives	1st caldera collapse	post-1st caldera eruptives	2nd collapse	post-2nd collapse eruptives
Menengai (McCall 1957, 1967)	Porphyritic peralkaline trachyte lava with several intervening old land surfaces. Topmost unit is a trachytic ignimbrite. Primitive cone has convex profile.	Elongate ENE long axis of 10–11 km. Age *ca.* 10 000 a B.P. Eruption of pumice and ash containing syenite nodules approx. coeval with caldera formation.	Peralkaline trachyte lavas erupted mainly within confines of caldera. Most recent eruption was within last century.		
Suswa (Johnson 1969)	Sodalite-bearing, peralkaline phonolite lavas. Primitive shield has a longer ENE axis of 20 km and a shorter axis of 17 km.	Elongate ENE long axis of 12 km. Eurption of early pumice and ash approx. coeval with caldera formation. Ring feeder lava eruptions then followed, accompanied by further pumice eruptions.	Early group of non-porphyritic lavas. Later group of porphyritic lavas formed a lava cone over 500 m above partly filled caldera floor.	Formation of pit crater, 1.6 km in diameter, at summit of lava cone, followed by collapse annual ring graben on caldera floor, slightly towards SE caldera rim.	Eruption of lava *ca.* 100–300 a B.P. in annular trench of ring graben.
Longonot (this paper)	Peralkaline trachyte lava and pyroclastics form a composite-volcano structure, basal diameter *ca.* 30 km.	Possible ENE long axis of *ca.* 7.5 km, although eastern half of caldera is buried by later eruptives. Eruption of pyroclastics with a minimum age of 9500 a B.P., coeval with caldera formation. These pyroclastics, and the syn-caldera pyroclastics of Suswa are in a similar state of erosion.	Eruption of mixed hawaiite –peralkaline trachyte lava followed by trachyte flows that formed a broad lava pile on the eastern caldera floor. Activity terminated by eruptions of ash and pumice.	Formation of pit crater, 1.8 km in diameter, at summit of lava pile.	Eruption of mixed lavas on pit-crater floor followed by eruption of peralkaline trachyte lava (*ca.* 200–300 a B.P.) from two radial fissures within the lava pile.

Longonot and Suswa both display an eastward migration of their major centres of activity.

to that of the early volcanoes at Longonot and Suswa, McCall (1967) believes that Menengai was active in the Pliocene.

(ix) Successive major centres of activity at Longonot and Suswa migrated eastwards with time, perhaps following lines of cross-faulting on the rift floor.

Comparison of all three major centres shows a possible overall similarity in the timing and shape of, and the activity associated with, the formation of the first calderas. When only Longonot and Suswa are compared, there are many more noticeable similarities in both the detailed histories of activity and the volcanic structures produced. In one respect, however Longonot is unique; it is the only centre on which mixed basic–felsic lavas have been identified, these being the first extrusive products erupted after each major collapse event. A similar association with caldera formation and faulting is reported by Weaver (1977) for basalts on the bimodal basalt–trachyte volcano Emuruangogolak in the north Kenya rift, but here mixing of the two end-members did not take place.

12. Conclusions

(1) The Quaternary volcano of Longonot is composed of peralkaline trachyte lavas and pyroclastics accompanied by minor volumes of mixed, hawaiite–peralkaline trachyte lava.

(2) Two major collapse events have taken place at Longonot. The first produced an embayed caldera, *ca.* 7.5 km in diameter, at the summit of an early composite volcano, while the second produced a circular pit crater, 1.8 km in diameter, at the summit of a later lava pile.

(3) Seven major rock units are distinguished:

(i) primitive, trachyte, composite-volcano eruptives;
(ii) syn- and post-caldera, trachyte pyroclastics;
(iii) northern plain, mixed lavas;
(iv) lava-pile trachytes;
(v) pre-pit-crater, trachyte ash;
(vi) post-pit-crater, mixed lavas;
(vii) recent, trachyte lavas.

(4) Mixed, hawaiite–peralkaline trachyte lavas are the first products to be erupted after each major collapse event.

(5) The major centre of activity has migrated eastwards with time, possibly following a cross fault on the rift floor.

(6) The syn- and post-caldera pyroclastics and the pre-pit-crater ash and pumice can be employed as marker horizons within the comendite volcanic succession of southwest Naivasha; this permits correlation of these volcanics with major eruptive episodes at Longonot.

(7) *At least* 20% of the total volume of liquid erupted at Longonot has been erupted in the form of pyroclasts; this emphasizes that at least 20% of the total sample suite should be pyroclastic. However, since their chemical composition is easily altered, a careful and critical approach to sampling is necessary to collect only those pyroclasts with a composition which is closest to that of the original liquid.

(8) Products formed from the greater part of the total liquid volume erupted at Longonot are not exposed; this creates a serious problem in the collection of a sample suite representative of liquid volumes erupted throughout the entire history of the volcano. Sampling of borehole

PHILOSOPHICAL TRANSACTIONS OF THE ROYAL SOCIETY A MATHEMATICAL, PHYSICAL & ENGINEERING SCIENCES

cores could partly alleviate the undersampling problem, but would risk production of a biassed sample suite, unrepresentative of the erupted liquid volumes.

(9) A sample suite truly representative of the erupted liquid volumes can only be collected from products erupted during and after the upper syn- and post-caldera pyroclastic activity. These products, however, account for only 14.5% of the total liquid volume erupted at the centre.

I warmly thank Professor D. K. Bailey for introducing me to the petrological problems of the Naivasha area and for his advice and encouragement at all stages of the work. Thanks are also due to Dr R. Macdonald for stimulating my interest in the Kenyan Quaternary volcanoes, to Dr M. K. Wells, Dr J. E. Guest and Dr A. M. Duncan for their authoritative discussion of volcanological problems and to Mr C. Stuart for drafting many of the diagrams. Dr G. P. L. Walker kindly read the initial draft of the manuscript and offered many suggestions for its improvement. Financial support from N.E.R.C. is gratefully acknowledged.

References

Baker, B. H. 1958 Geology of the Magadi area. *Rep. geol. Surv. Kenya*, no. 42.

Baker, B. H. & Mitchell, J. 1976 Volcanic stratigraphy and geochronology of the Kedong-Olorgesailie area and the evolution of the South Kenya rift valley. *J. geol. Soc. Lond.* **132**, 467–484.

Baker, B. H. & Wohlenberg, J. 1971 Structure and evolution of the Kenya Rift Valley. *Nature, Lond.* **229**, 538–542.

Booth, B. 1973 The Granadilla pumice deposit of southern Tenerife, Canary Islands. *Proc. Geol. Ass.* **84**, 353–370.

Crowe, B. M. & Fisher, R. V. 1973 Sedimentary structures in base surge deposits with special reference to cross bedding, Ubehebe Craters, Death Valley, California. *Bull. geol. Soc. Am.* **84**, 663–682.

Gregory, J. W. 1896 *The Great Rift Valley*. London: J. Murray.

Gregory, J. W. 1920 The African Rift Valleys. *Geogrl J.* **61**, 13–47.

Gregory, J. W. 1921 *The rift valleys and geology of East Africa*. London: Seeley Service and Co.

Johnson, R. W. 1969 Volcanic geology of Mount Suswa, Kenya. *Phil. Trans. R. Soc. Lond.* A **265**, 383–412.

Kamau, C. 1974 The Lake Naivasha basin. *Rep. geogr. Dep. Nairobi University*.

Lirer, L., Pescatore, T., Booth, B. & Walker, G. P. L. 1973 Two plinian pumice fall deposits from Somma–Vesuvius, Italy. *Bull. geol. Soc. Am.* **84**, 759–772.

McCall, G. J. H. 1957 Geology and groundwater conditions in the Nakuru area. *Tech. Rep. Kenya Ministry Works*, no. **13**.

McCall, G. J. H. 1967 Geology of the Nakuru–Thompson's Falls–Lake Hannington area. *Rep. geol. Surv. Kenya* **70**.

Moore, J. G. 1967 Base surge in recent volcanic eruptions. *Bull. volcan.* **30**, 337–363.

Richard, J. J. & Neumann Van Padang, M. 1957 *Catalogue of active volcanoes of the world including solfatara fields. IV. Africa and the Red Sea*. Naples: Int. Ass. Volcan.

Richardson, J. L. & Richardson, A. E. 1972 History of an African Rift lake and its climatic implications. *Ecol. Monogr.* **42**, 499–534.

Rittman, A. 1962 Erkläuungsversuch zum Mechanismsus der Ignimbritausbruche. *Geol. Rdsch.* **52**, 853–861.

Schmincke, H. U., Fisher, R. V. & Waters, A. C. 1973 Antidune and shute pool structures in the base surge deposits of the Laacher See area, Germany. *Sedimentology* **20**, 553–574.

Shackleton, R. M. 1955 Pleistocene earth movements in the Gregory Rift Valley. *Geol. Rdsch.* **43**, 257–263.

Sparks, R. S. J. & Walker, G. P. L. 1973 The ground surge deposit; a third type of pyroclastic rock. *Nature, Lond.* **241**, 62–64.

Sparks, R. S. J. & Wilson, L. 1976 A model for the formation of ignimbrite by gravitational column collapse. *J. geol. Soc. Lond.* **132**, 441–452.

Thompson, A. O. & Dodson, R. G. 1963 Geology of the Naivasha area. *Rep. geol. Surv. Kenya*, no. 55.

Walker, G. P. L. 1973 The imbalance between volcanology and geochemistry. *Q. Jl geol. Soc. Lond.* **129**, 648.

Waters, A. C. & Fisher, R. V. 1970 Base surge bed forms in marr volcanoes. *Am. J. Sci.* **268**, 157–170.

Weaver, S. D. 1977 The Quaternary caldera volcano Emuruangogolak, Kenya Rift, and the petrology of a bimodal ferrobasalt–pantelleritic trachyte association. *Bull. volcan.* **40**, 1–22.

PHILOSOPHICAL TRANSACTIONS OF THE ROYAL SOCIETY A MATHEMATICAL, PHYSICAL & ENGINEERING SCIENCES

THE VOLCANIC GEOLOGY OF MOUNT LONGONOT, CENTRAL KENYA

S.C. Scott, 1979

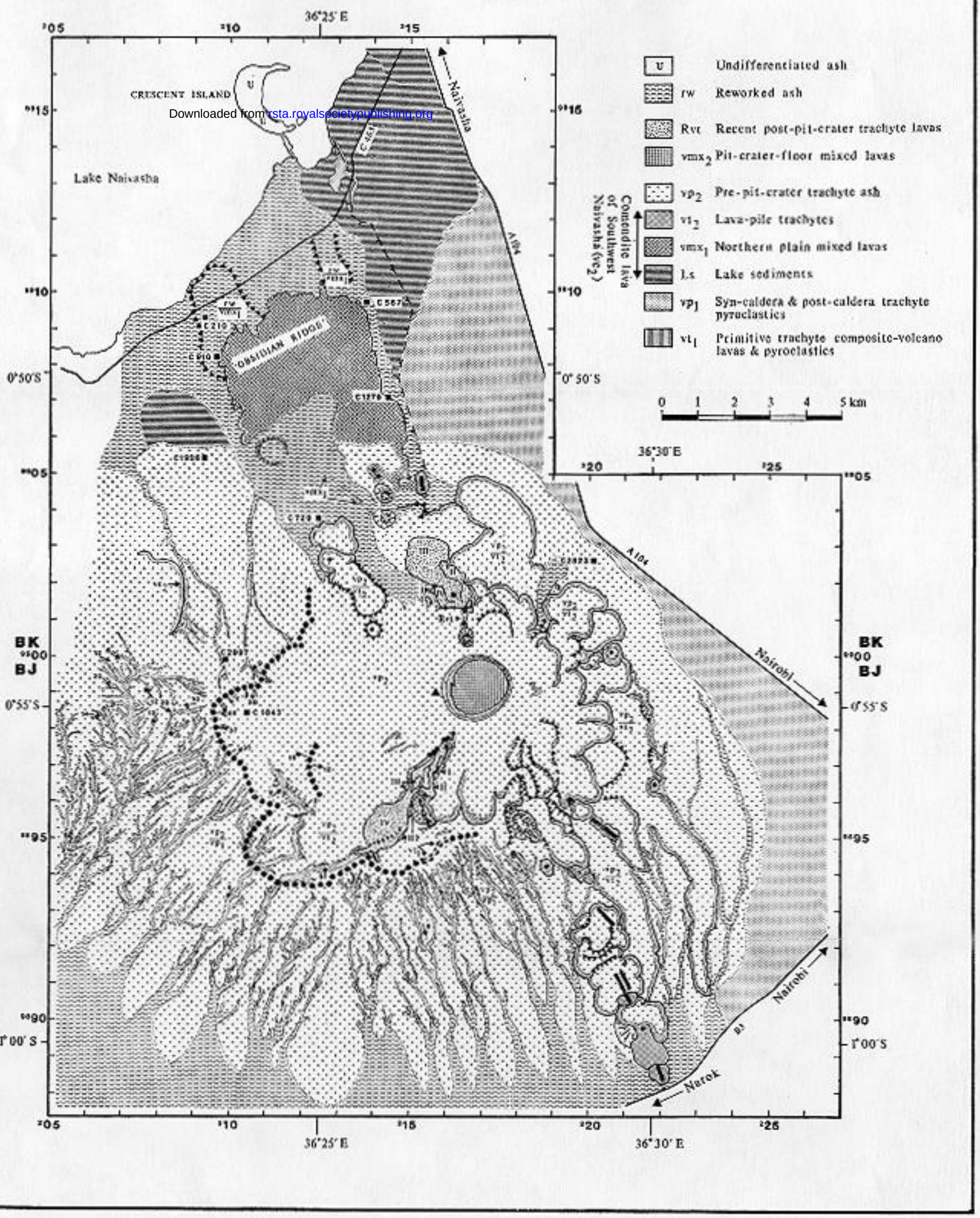

FIGURE 2.

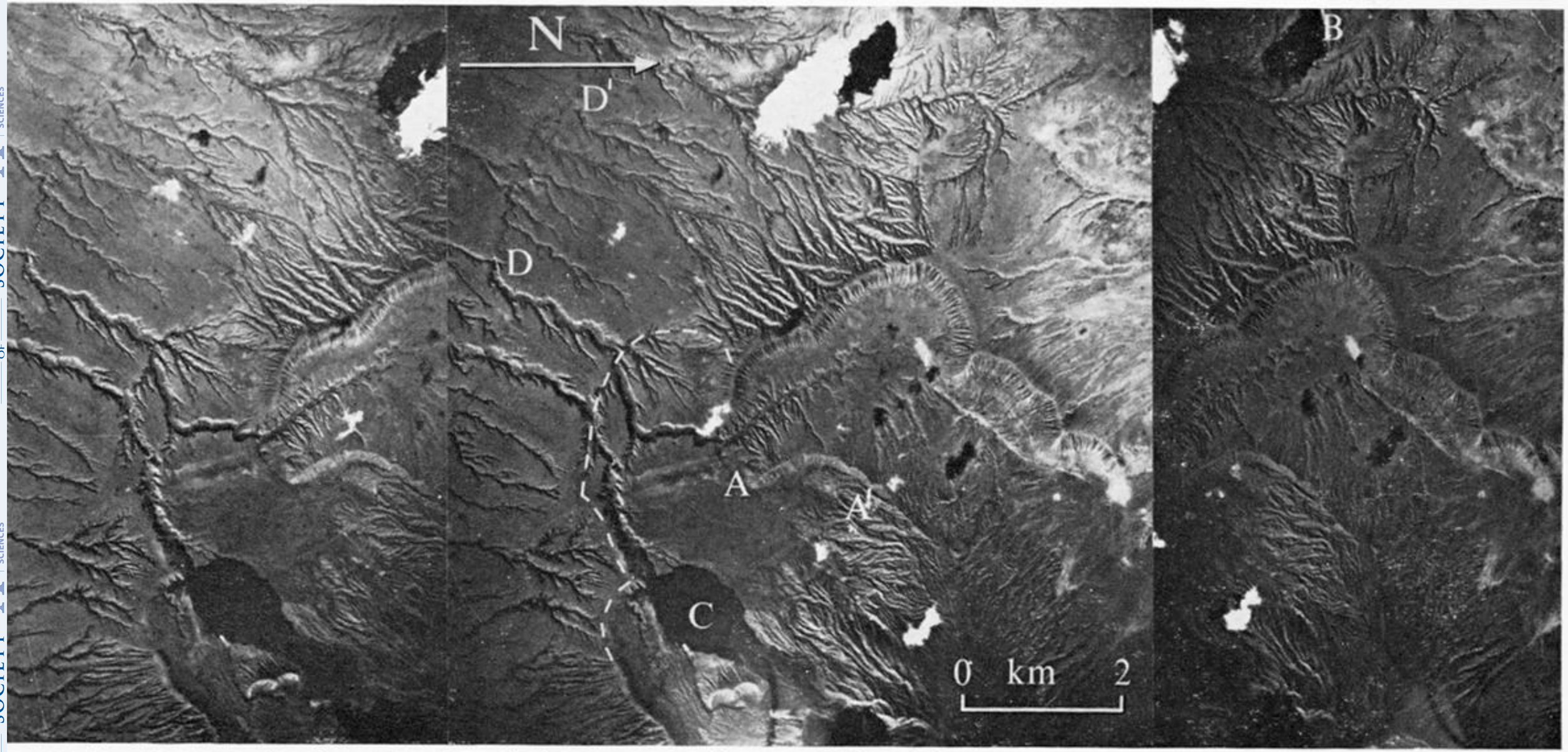

IGURE 4. Stereo air photographs of the pyroclastic-mantled caldera scarp. Dashed white line indicates the position of the scarp where it is topographically ill defined; A–A′, arcuate, pyroclastic-mantled remnant of collapsed composite-volcano summit region; B, pyroclastic-mantled cone structures; C, recent southwest flank flow; D–D′, linear feature of unknown origin. (Survey of Kenya photographs V13A 1072, 088–090.)

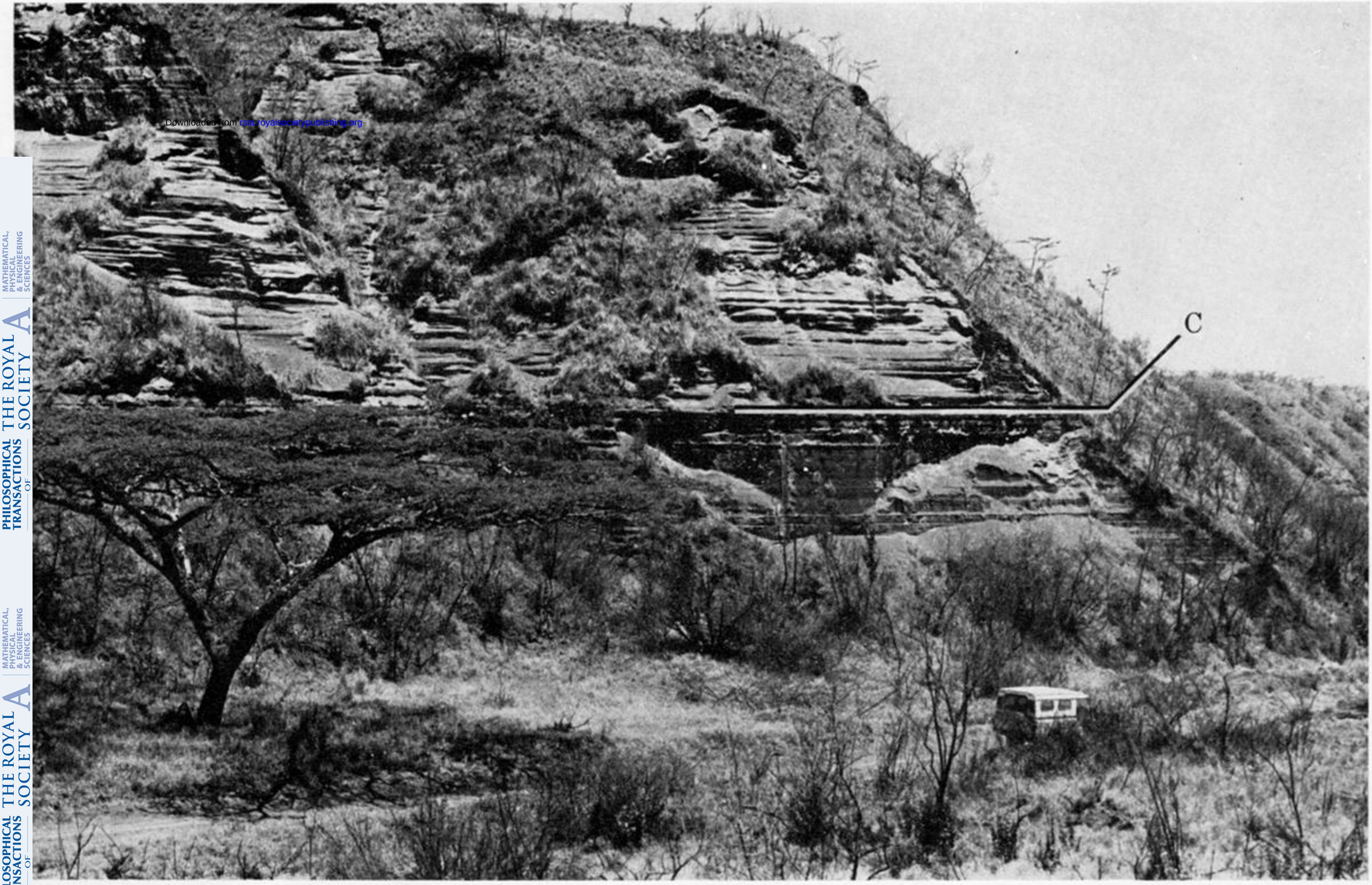

IGURE 10. Contact, C, between Unit III airfall–pumice beds (below C) and Unit IV airfall–ash beds (above C) exposed at BJ115965. (Landrover at bottom, right, gives scale.)

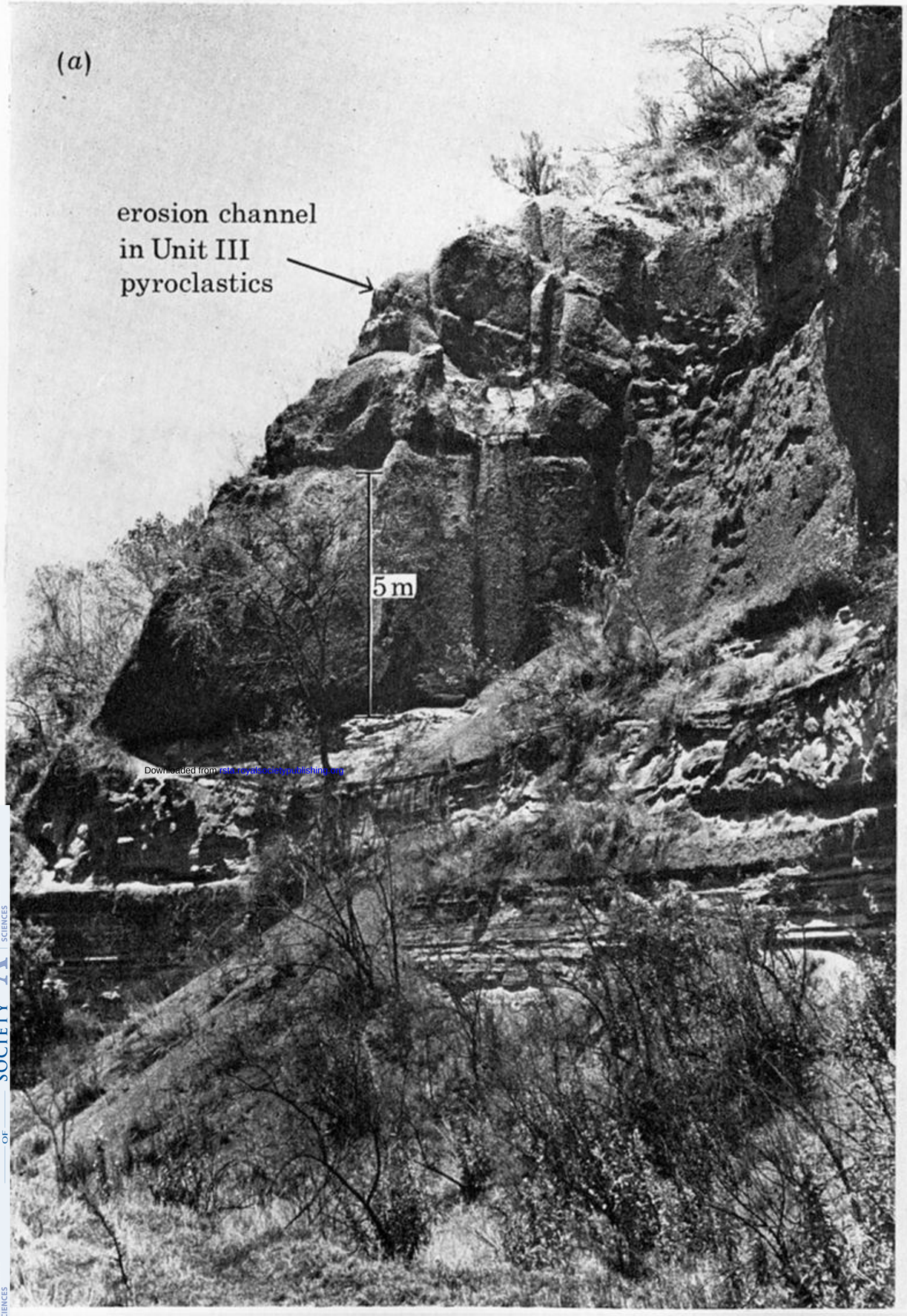

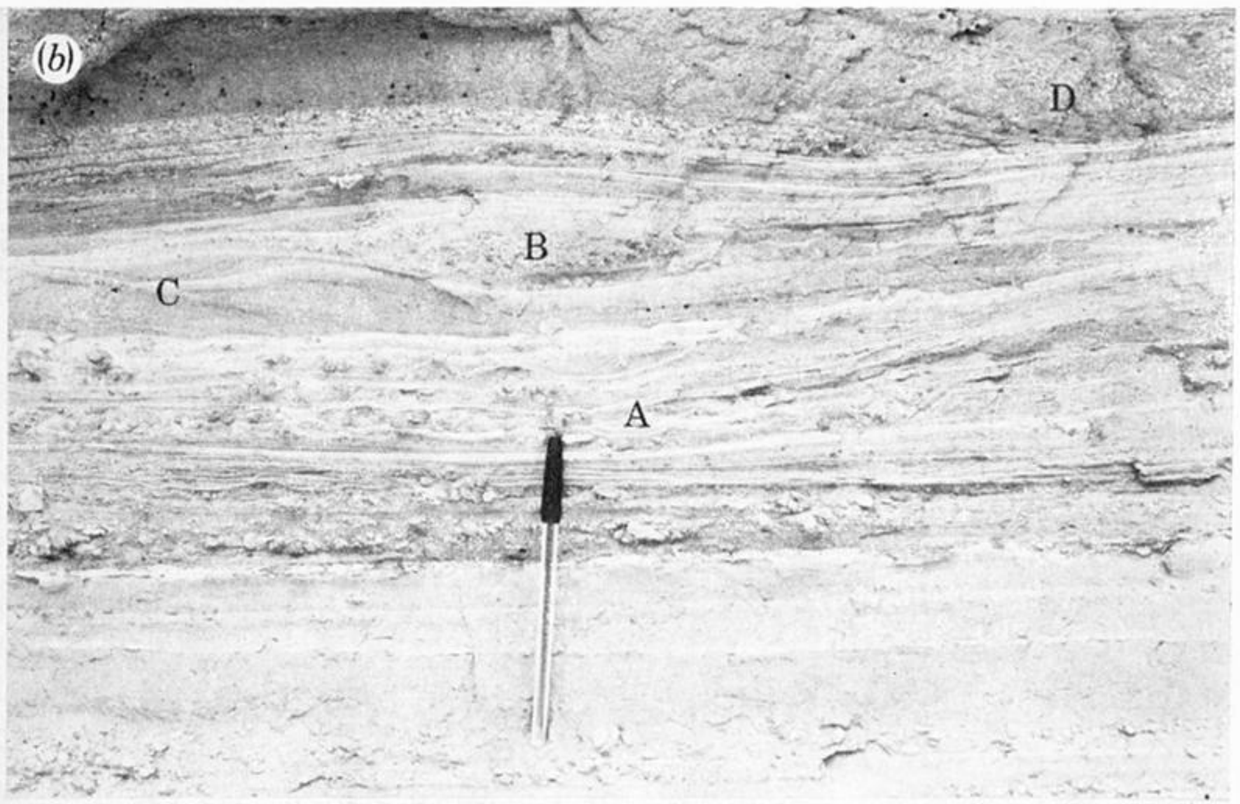

Unit III

Unit II

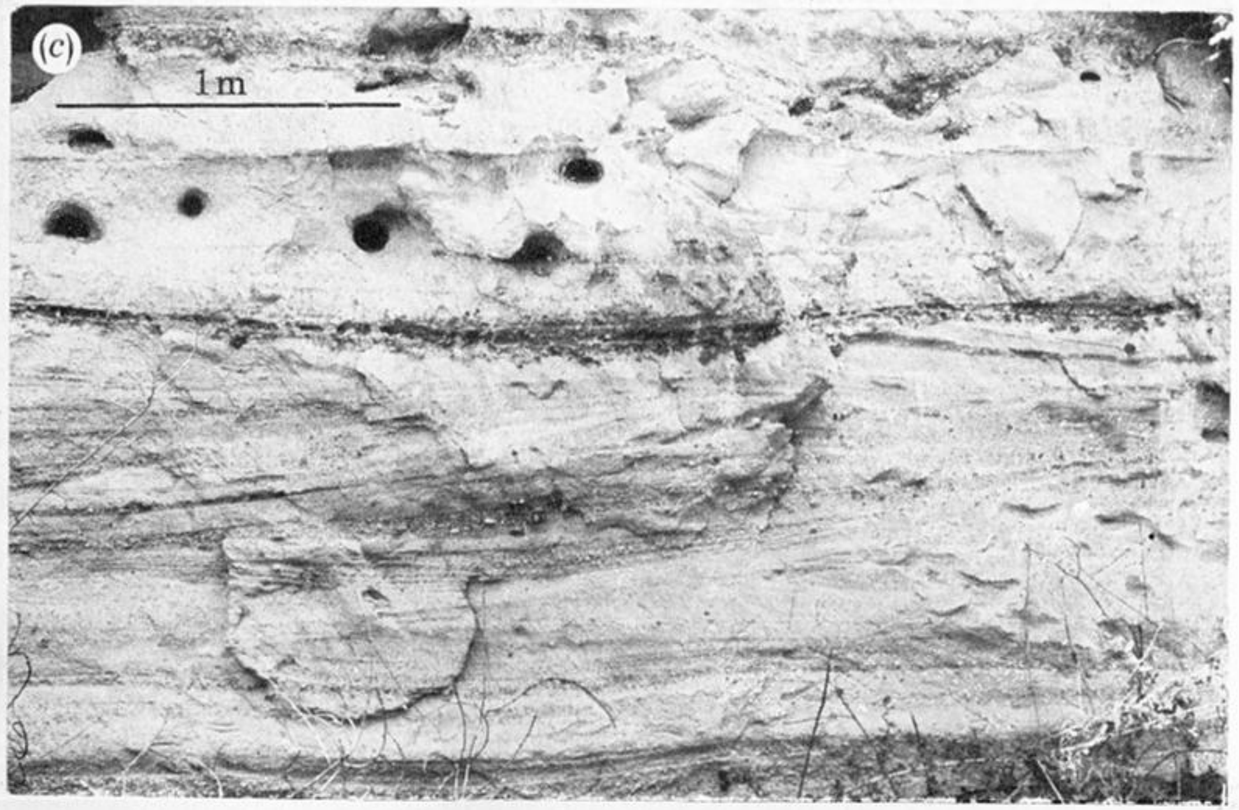

FIGURE 9. (*a*) Type section for the syn- and post-caldera, Unit II pyroclastic deposit exposed at BJ110944. Also visible is the lower part of the overlying Unit III succession which, at this locality, exposes part of an infilled erosion channel.

(*b*) Structures in the base-surge deposit exposed at BJ110944 (see figure 8 for position in type section). A parallel-laminated surge unit is overlain by a unit exhibiting dune cross-bedding. Fine laminations deformed by, and around, larger clasts are seen on the leeside of a dune at A. Possible shute and pool structure at B. Stoss-side slopes, preserved at C and D, are built up from the surface of the lee slope of an underlying dune. Flow is from right to left. Scale: pen length = 15 cm.

(*c*) Structures in base-surge deposit exposed at BJ119946 (see figure 8 for position in type section). Poorly sorted, cross-bedded ash and lapilli horizons are shown in the lower part of the photograph. A poorly sorted, sinuous lapilli horizon with a wavelength of 2.5 m and amplitude of 0.15 m is shown in the upper part of the photograph. Flow is from left to right.

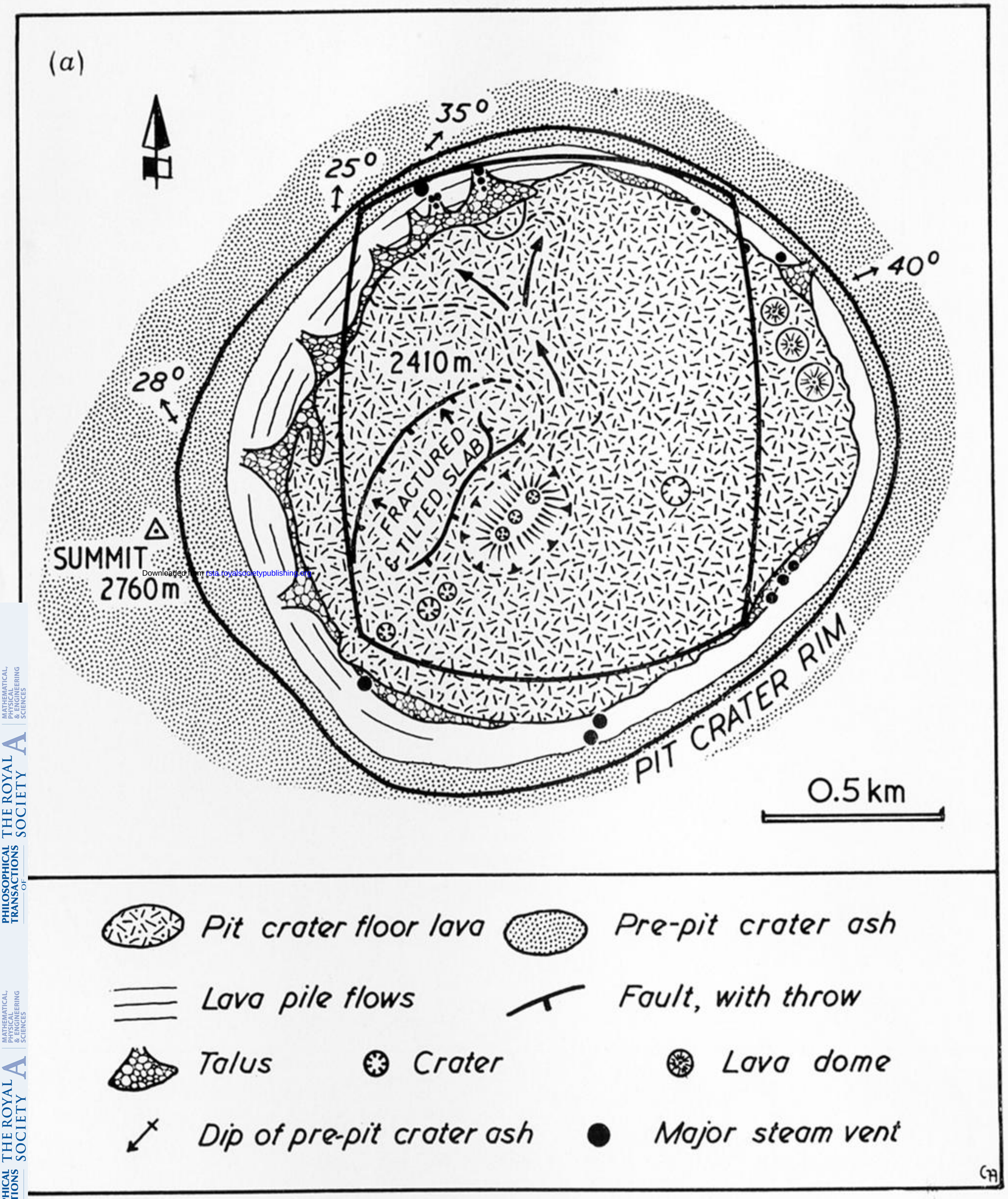

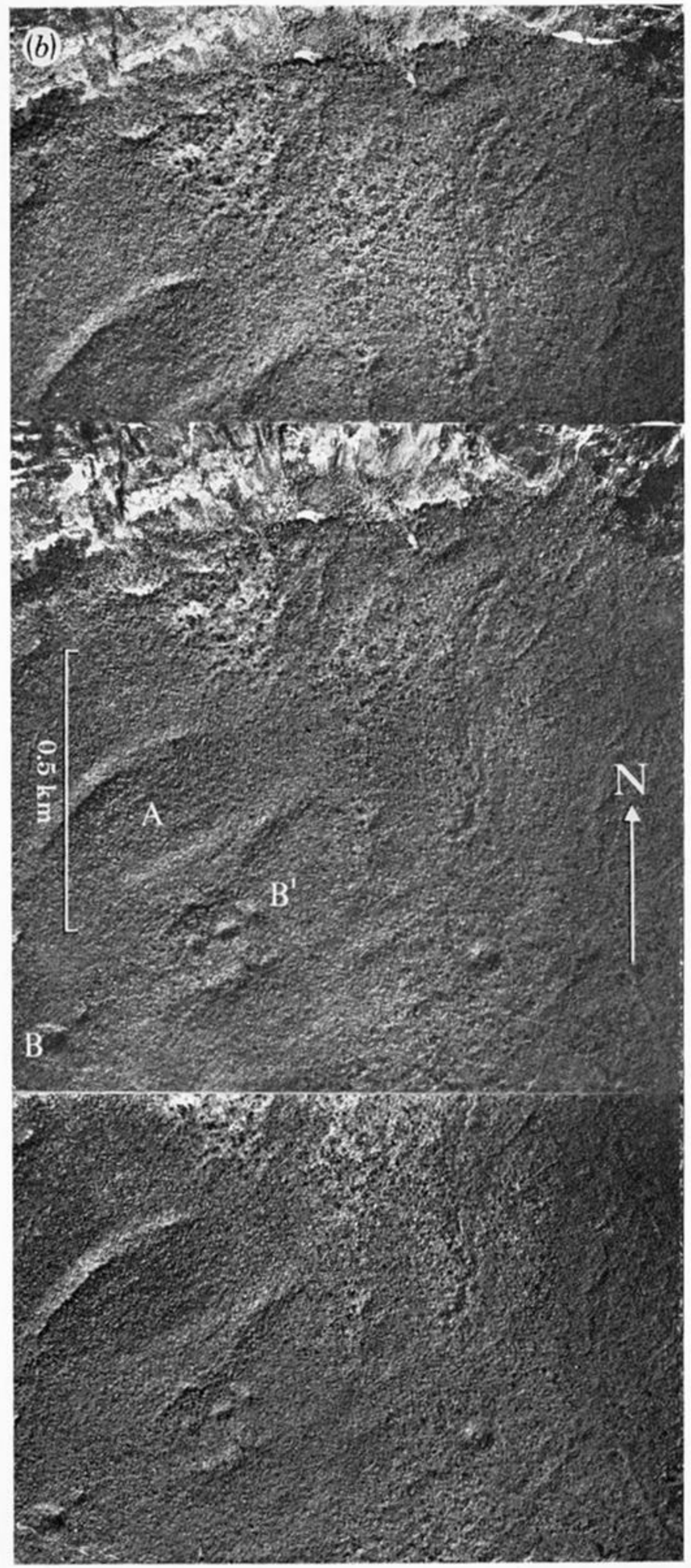

FIGURE 13. (*a*) Photogeological sketch map of the pit-crater floor. (*b*) Stereo air photographs of part of the pit-crater floor delimited by the enclosed area on figure 13*a*. A, fractured and tilted slab; B–B′, crater alignment. (Survey of Kenya photographs 69/90, 153–155.)